

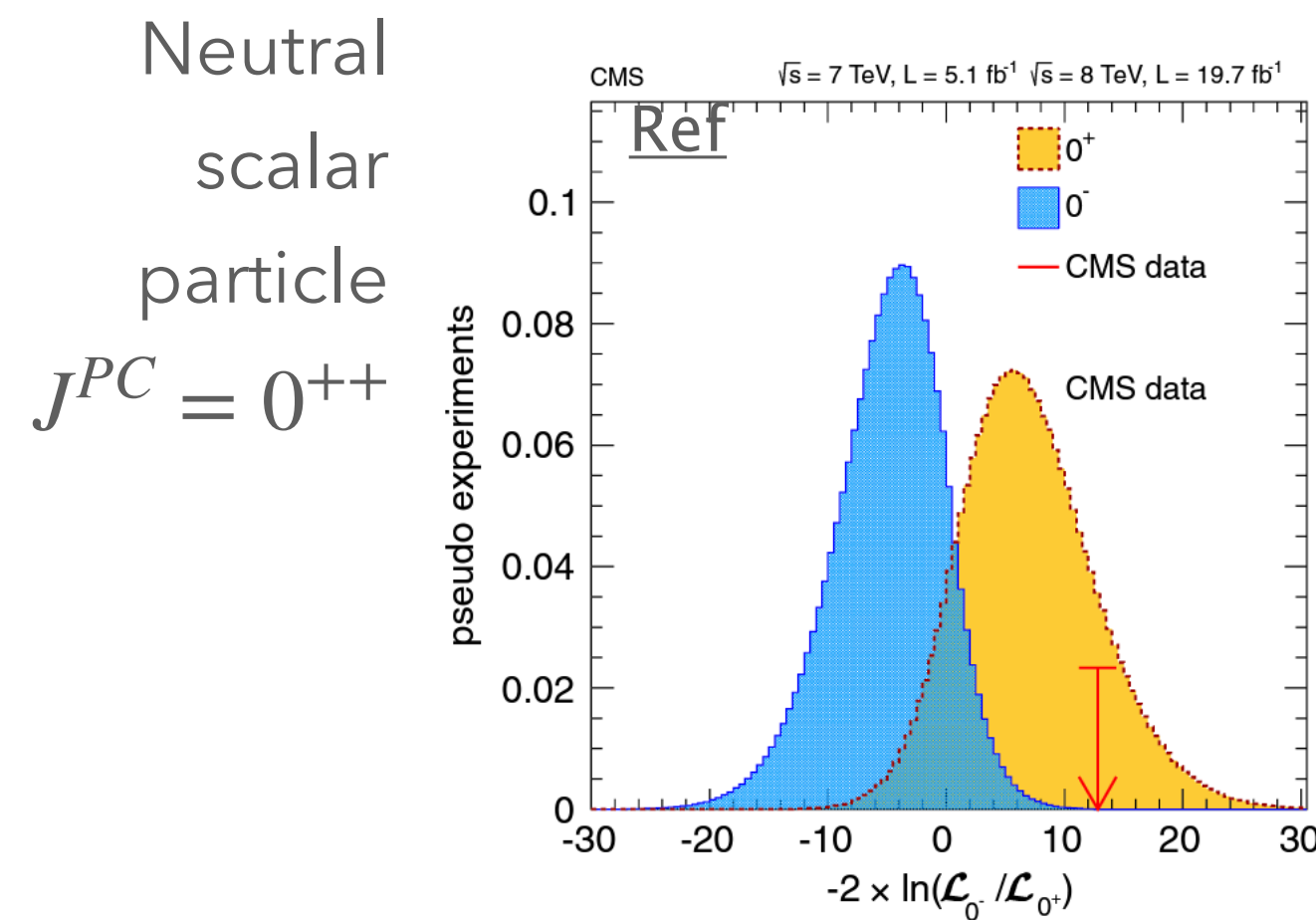
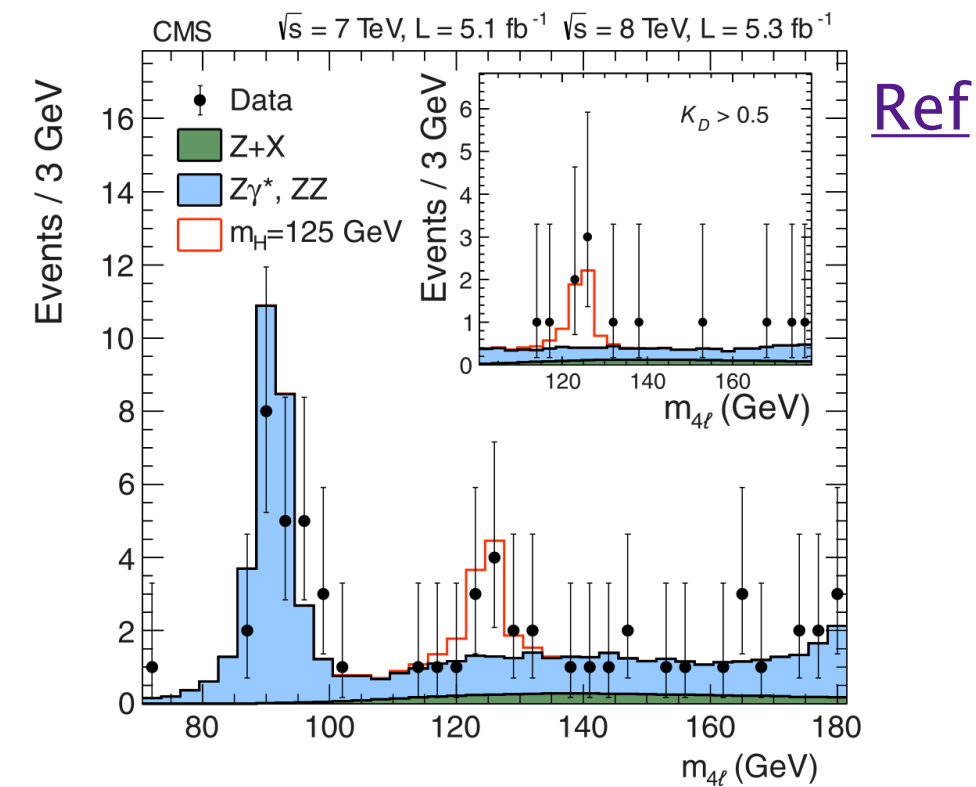
CONSTRAINTS ON ANOMALOUS HIGGS BOSON COUPLINGS TO VECTOR BOSONS AND FERMIONS IN THE $\gamma\gamma$ FINAL STATE



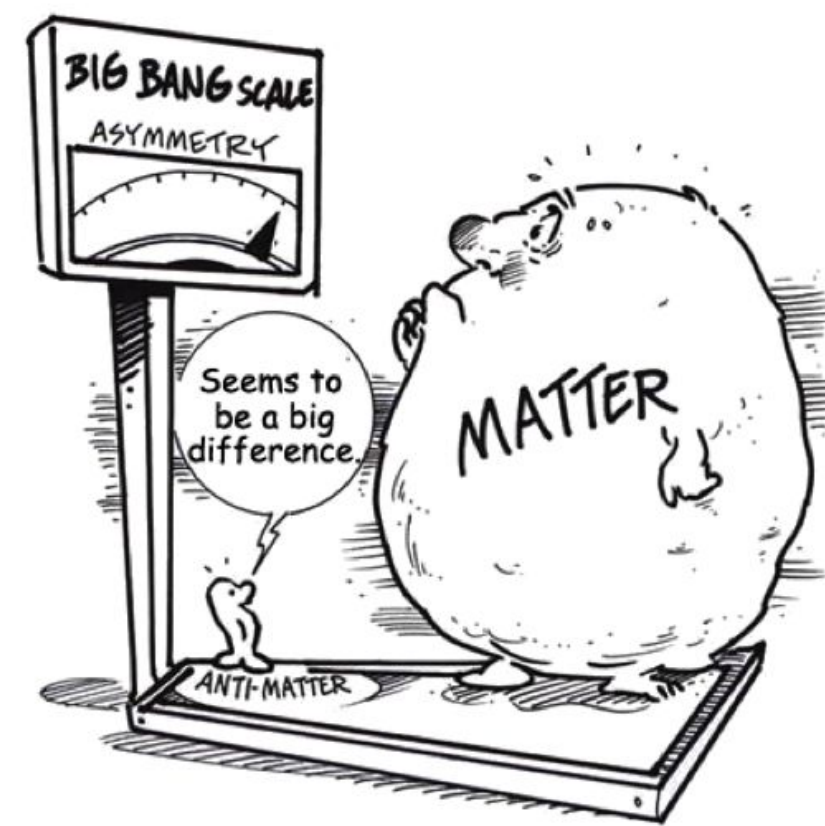
Federica De Rigi on behalf of the CMS
collaboration

Higgs Hunting 2025

Higgs Boson Properties

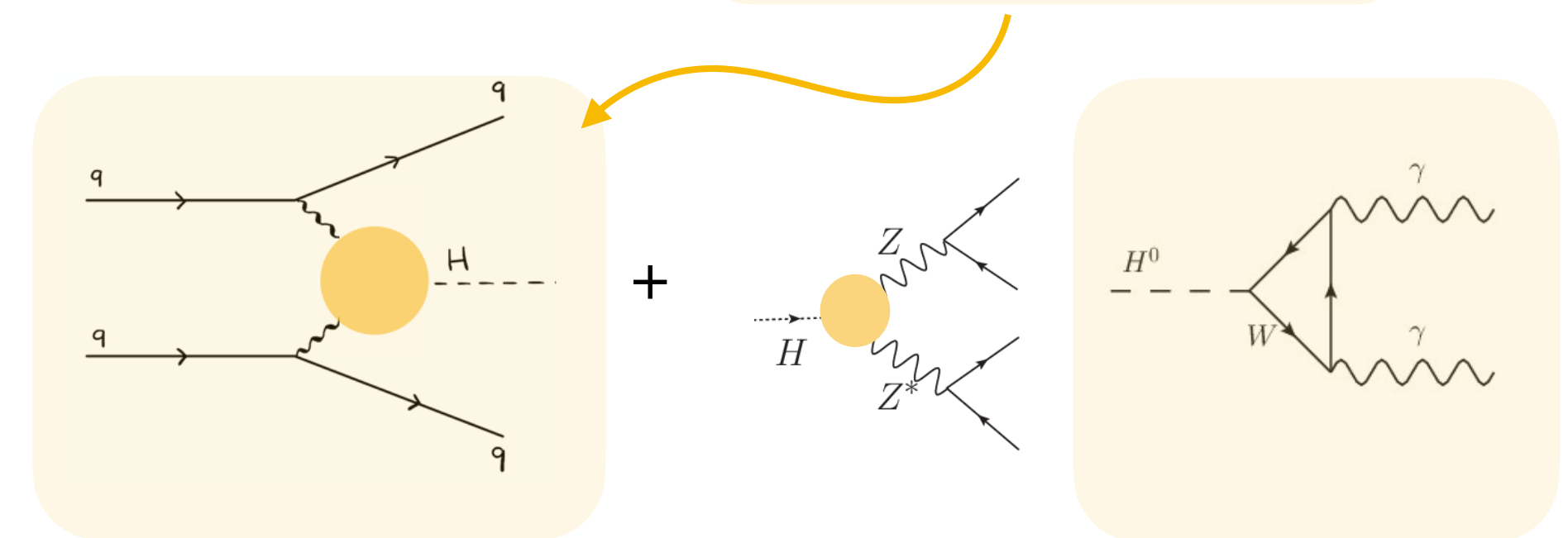


What happened to antimatter? The asymmetry between matter and antimatter implies CP violation. The Standard Model (SM) can only partially explain the CP violation needed \rightarrow we look for other sources of violation \rightarrow search for anomalous couplings (AC)



Anomalous coupling searches started from $H \rightarrow ZZ \rightarrow 4\ell$ (both production and decay couplings)

Sensitivity improves thanks to access to larger, q^2 values ($q^2 > M_H^2$), where BSM effects are enhanced, when using production coupling.



Since the main sensitivity comes from production, the $\gamma\gamma$ final state becomes an ideal choice due to its high efficiency and excellent mass resolution, which allow for effective background suppression

Discovery

MORE-DATA

BSM research

AC $H \rightarrow ZZ$ AC $H \rightarrow \gamma\gamma$

Anomalous couplings

$$A(HVV) \sim \left[a_1^{VV} + \frac{k_1^{VV} q_{V1}^2 + k_2^{VV} q_{V2}^2}{(\Lambda_1^{VV})^2} \right] m_{V1}^2 \epsilon_{V1}^* \epsilon_{V2}^* + a_2^{VV} f_{\mu\nu}^{*(1)} f^{*\mu\nu(2)} + a_3^{VV} f_{\mu\nu}^{*(1)} \tilde{f}^{*\mu\nu(2)}$$

CP even CP odd

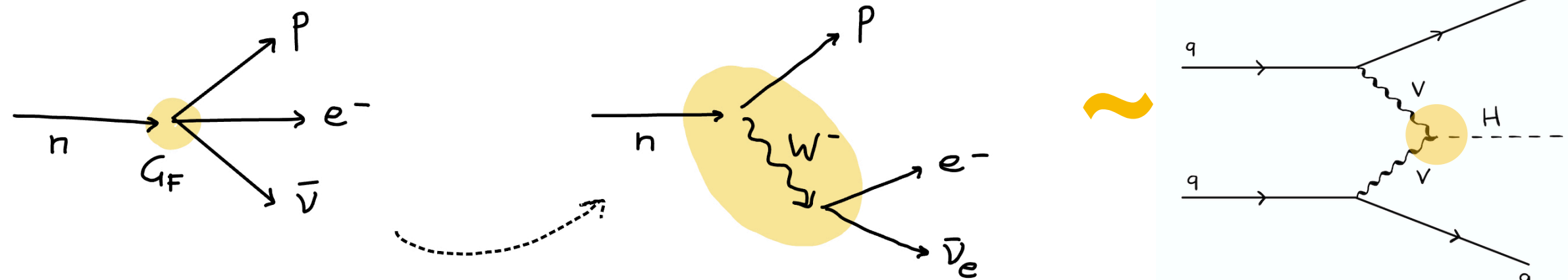
Tree level contribution
 $a_1\gamma\gamma = a_1gg = a_1Z\gamma = 0$
 Custodial symmetry
 $a_1ZZ = a_1WW$

SM

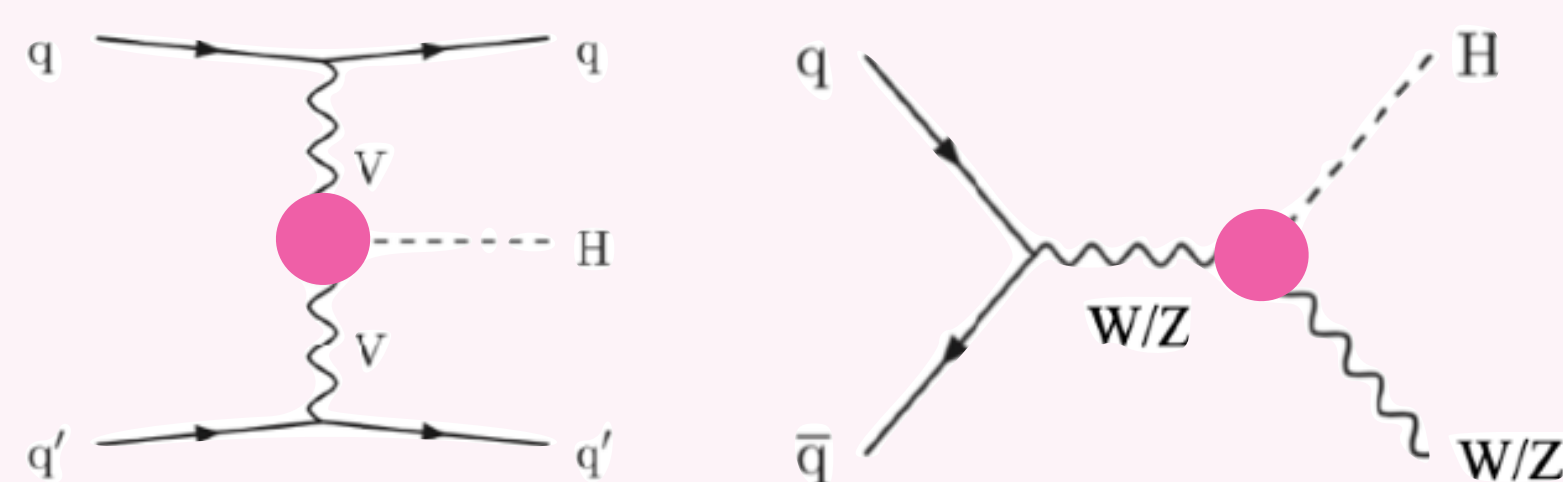
Symmetry and gauge invariance
 properties require

$$k_iZZ = k_iWW, k_i\gamma\gamma = k_2\gamma\gamma = k_1gg = k_2gg = k_1Z\gamma = 0$$

New physics scale ($\Lambda_1 = 1\text{TeV}$)



HVV
 COUPLING :
 $V = WW, ZZ$



Four couplings from each term

- ▶ a_1^{VV} CP even, SM-like (=2)
- ▶ a_2^{VV} CP even
- ▶ a_3^{VV} CP odd
- ▶ Λ_1

**Four anomalous coupling
 parameters:**

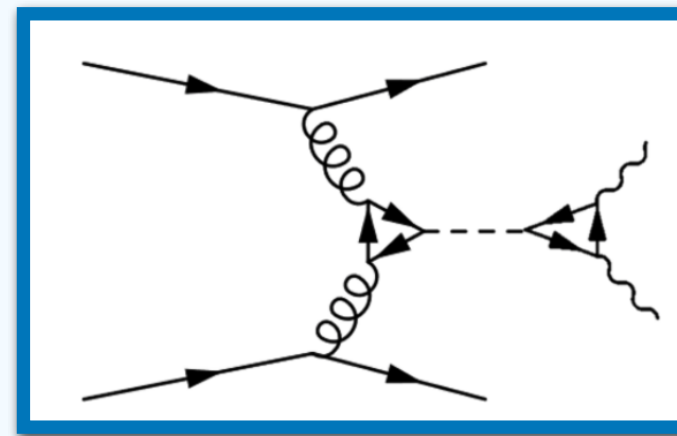
$$a_2, a_3, \Lambda_1, \Lambda_1^{Z\gamma}$$

Anomalous couplings

$$A(HVV) \sim \left[a_1^{VV} + \frac{k_1^{VV} q_{V1}^2 + k_2^{VV} q_{V2}^2}{(\Lambda_1^{VV})^2} \right] m_{V1}^2 \epsilon_{V1}^* \epsilon_{V2}^* + a_2^{VV} f_{\mu\nu}^{*(1)} f^{*\mu\nu(2)} + a_3^{VV} f_{\mu\nu}^{*(1)} \tilde{f}^{*\mu\nu(2)}$$

CP even
SM
CP odd

Hgg COUPLING : V = gg

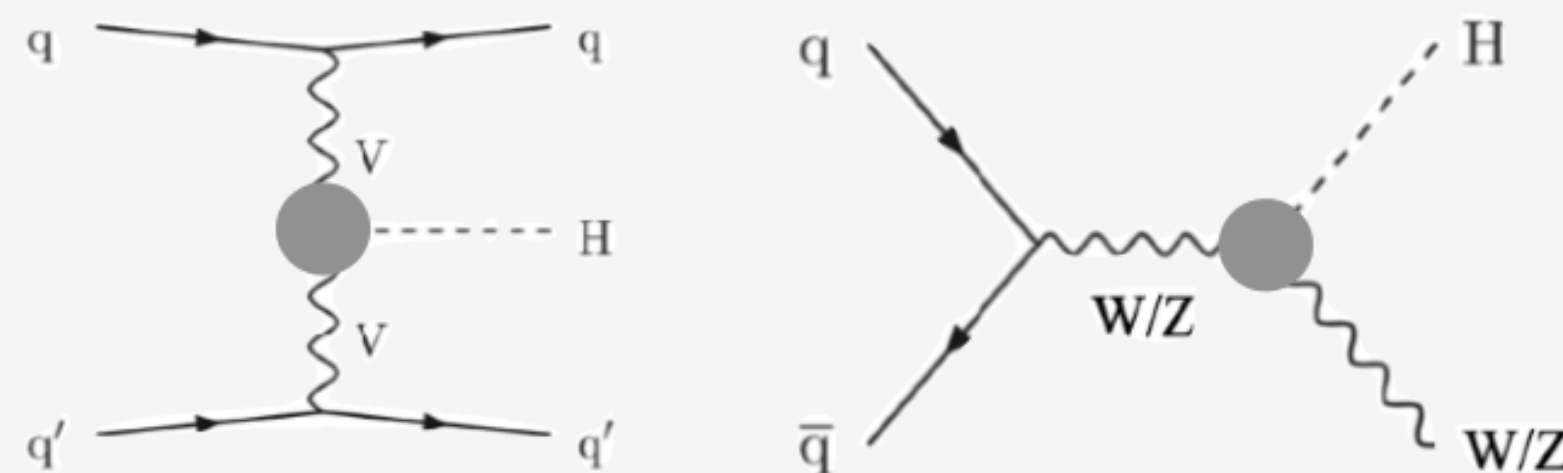


Two coupling from 2nd & 3rd term

- ▶ a_2^{VV} CP even, SM-like
- ▶ a_3^{VV} CP odd

One anomalous coupling: a_3^{ggH}

HVV
COUPLING :
V = WW, ZZ



Four couplings from each term

- ▶ a_1^{VV} CP even, SM-like (=2)
- ▶ a_2^{VV} CP even
- ▶ a_3^{VV} CP odd
- ▶ Λ_1

Four anomalous coupling parameters:
 $a_2, a_3, \Lambda_1, \Lambda_1^{Z\gamma}$

Anomalous couplings

$$A(HVV) \sim \left[a_1^{VV} + \frac{k_1^{VV} q_{V1}^2 + k_2^{VV} q_{V2}^2}{(\Lambda_1^{VV})^2} \right] m_{V1}^2 \epsilon_{V1}^* \epsilon_{V2}^* + a_2^{VV} f_{\mu\nu}^{*(1)} f^{*\mu\nu(2)} + a_3^{VV} f_{\mu\nu}^{*(1)} \tilde{f}^{*\mu\nu(2)}$$

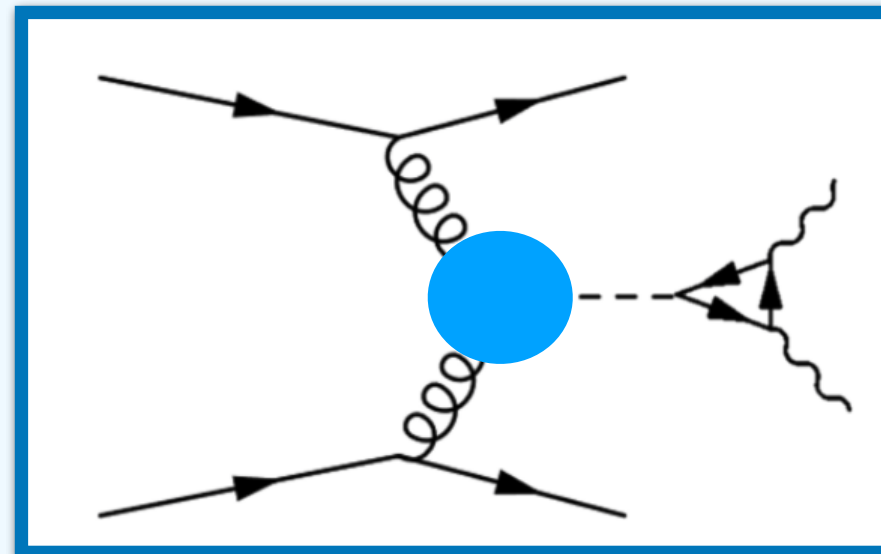
Parametrization: Effective cross section fractions

► **HVV COUPLING** $a_2, a_3, \Lambda_1, \Lambda_1^{Z\gamma}$ parametrized:

$$\mu_V, \mu_f \quad \& \quad f_{ai} = \frac{|a_i|^2 \sigma_i}{\sum_{j=1,2,3,\Lambda_1} |a_j|^2 \sigma_j} \text{sgn}\left(\frac{a_i}{a_1}\right)$$

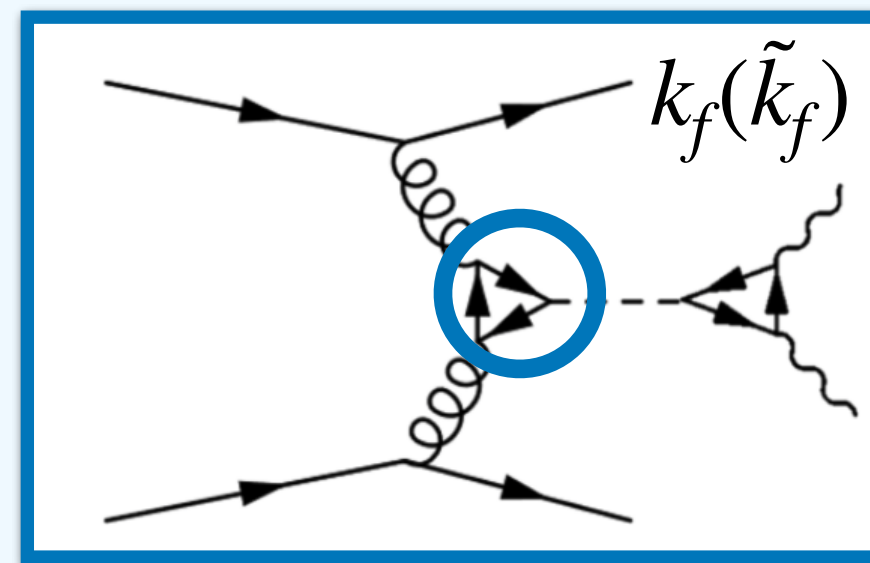
► **Hgg COUPLING** a_3^{ggH} parametrized:

$$\mu_f, \mu_V, f_{a3} \quad \& \quad f_{a3}^{ggH} = \frac{|a_3^{gg}|^2}{|a_2^{gg}|^2 + |a_3^{gg}|^2} \text{sgn}\left(\frac{a_3^{gg}}{a_2^{gg}}\right)$$



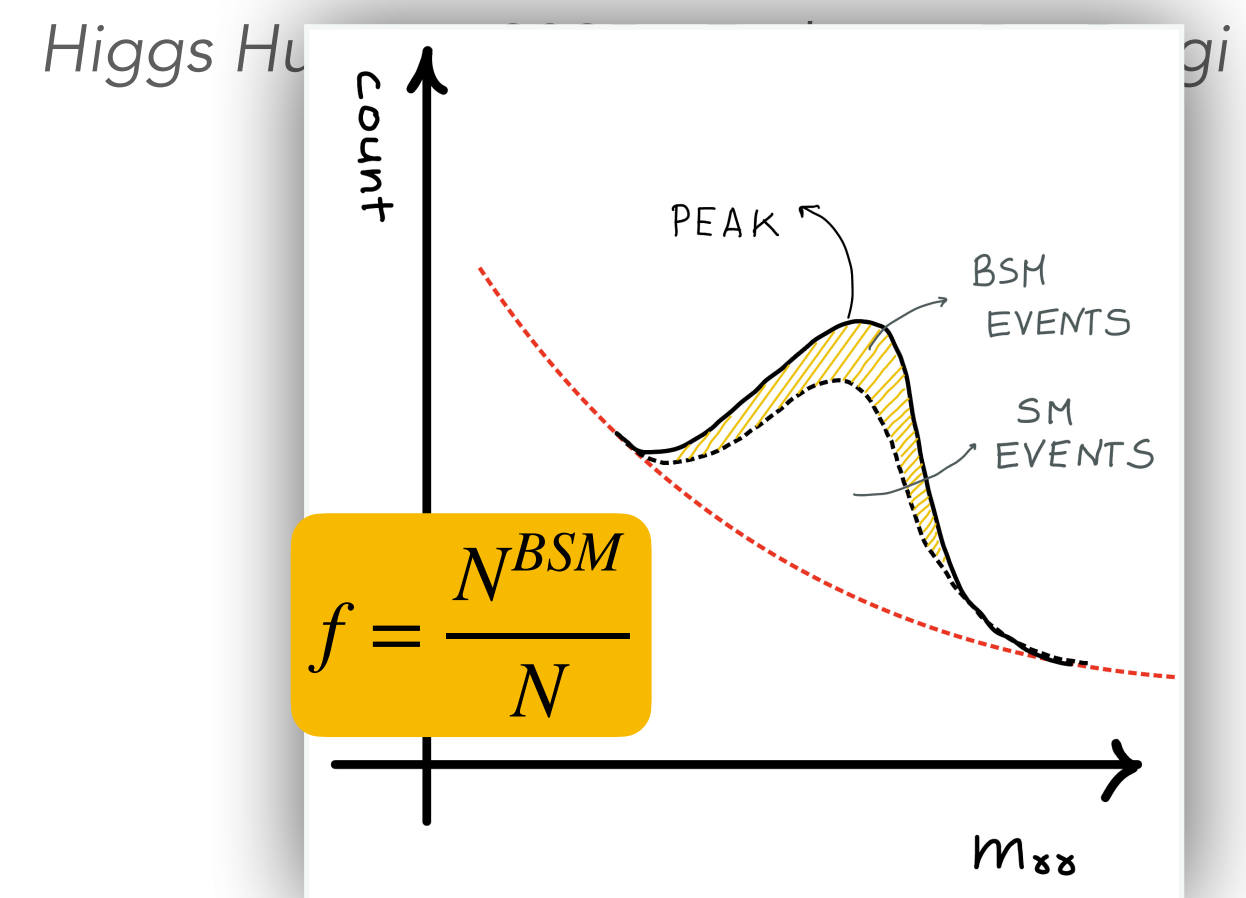
By studying the interaction of the Higgs boson with gluons (Hgg), we can probe the anomalous CPodd interaction between Higgs and fermions indirectly

Generic Hff scattering amplitude



$$A(Hff) = -\frac{m_f}{v} \bar{\psi}_f (\kappa_f + i \tilde{\kappa}_f \gamma_5) \psi_f,$$

$$|f_{CP}^{Hff}| = \left(1 + 2.38 \left[\frac{1}{|f_{a3}^{ggH}|} - 1 \right] \right)^{-1}$$



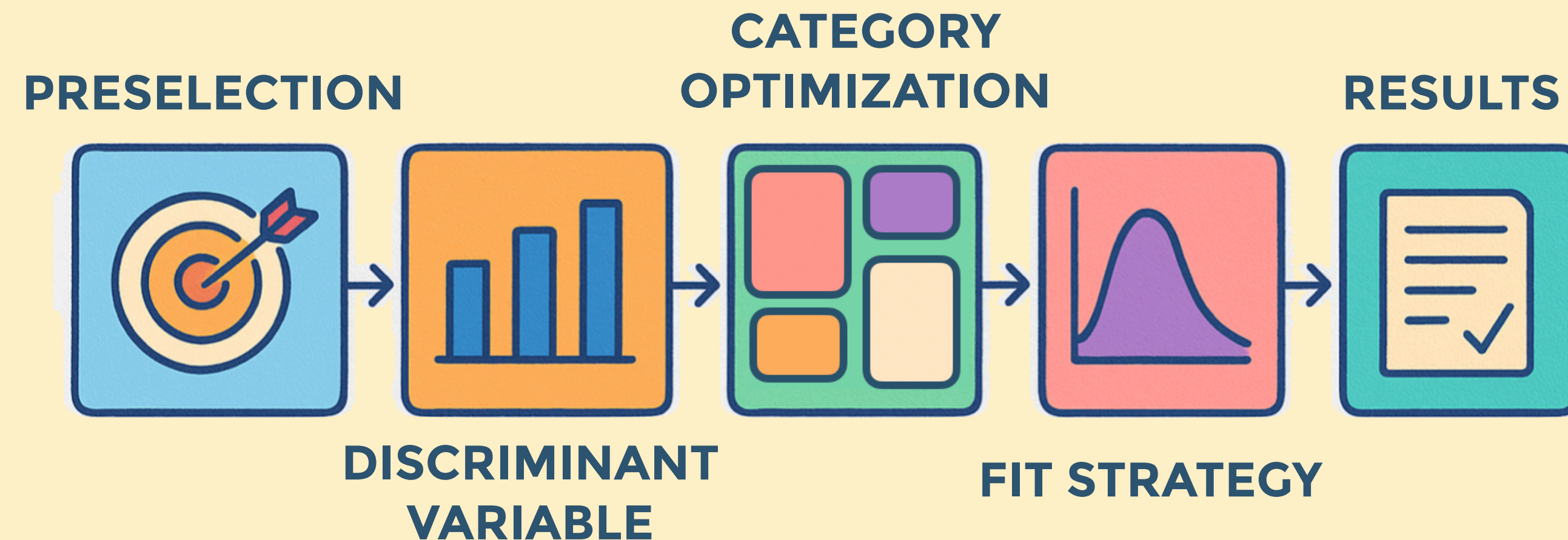
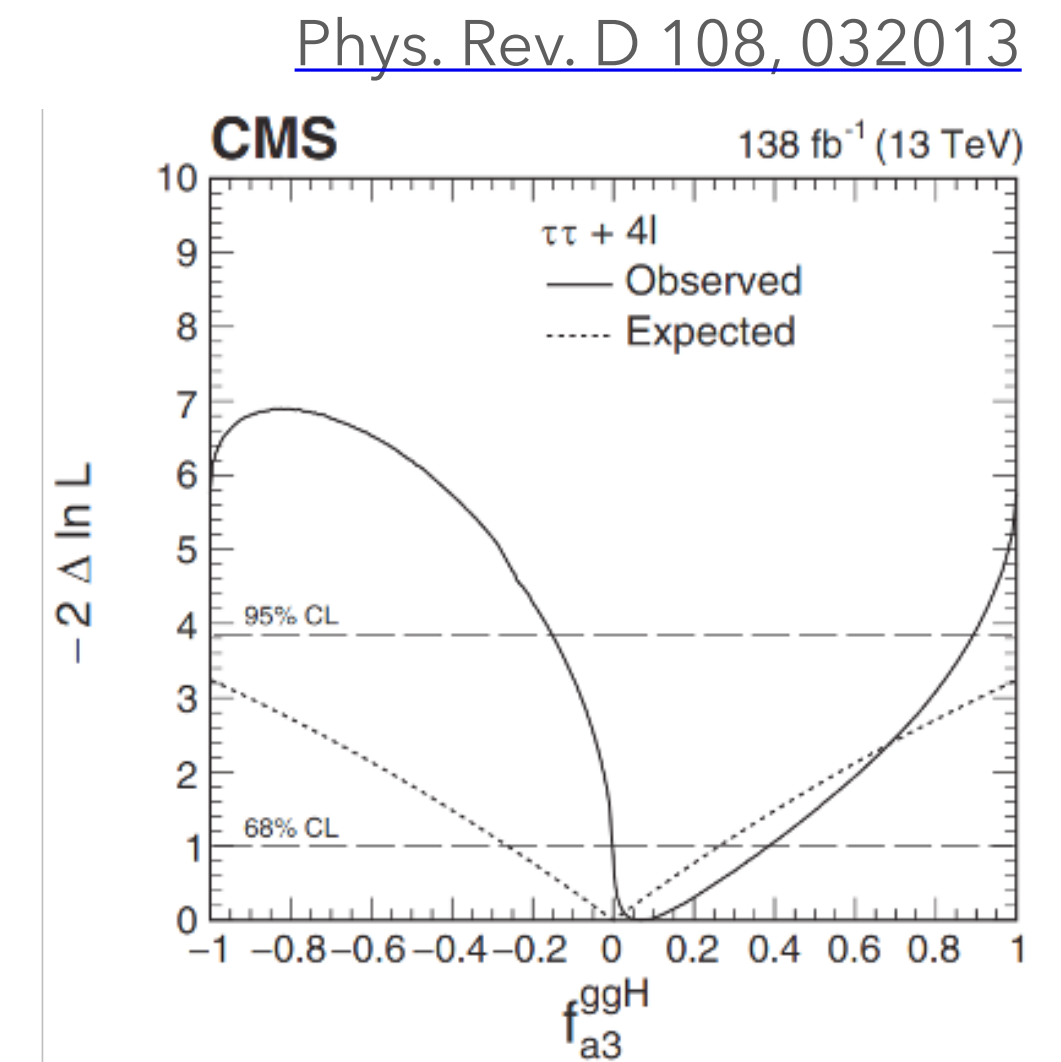
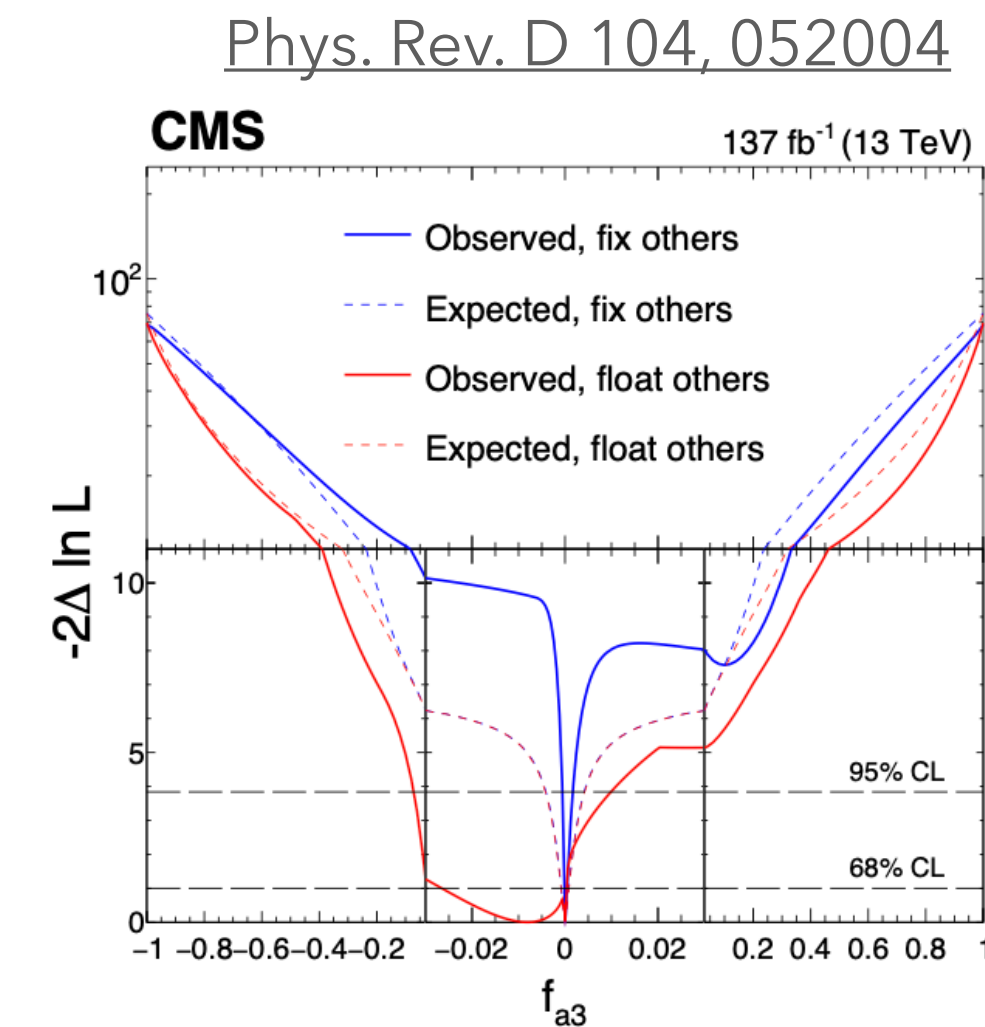
* σ_i = cross section for the process corresponding to $a_i = 1$

Analysis strategy

Comprehensive studies of CP violation, anomalous couplings, and the tensor structure of Higgs have been performed previously with other Higgs decay channel

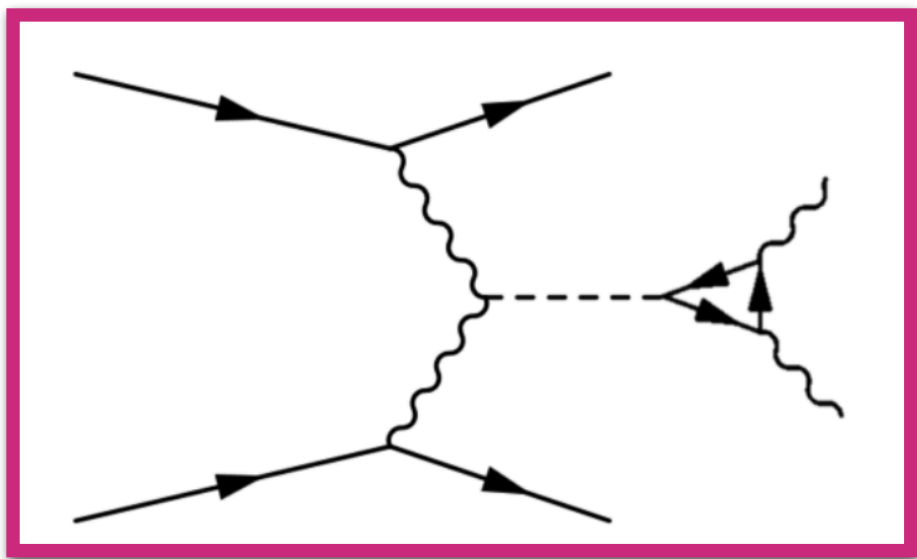
- [Phys. Rev. D 104, 052004](#) : $H \rightarrow 4\ell$
- [Phys. Rev. D 108, 032013](#) : $H \rightarrow \tau\tau$ (with result of $H \rightarrow 4\ell + H \rightarrow \tau\tau$)
- [Eur. Phys. J. C 84 \(2024\) 779](#) : $H \rightarrow WW$

+

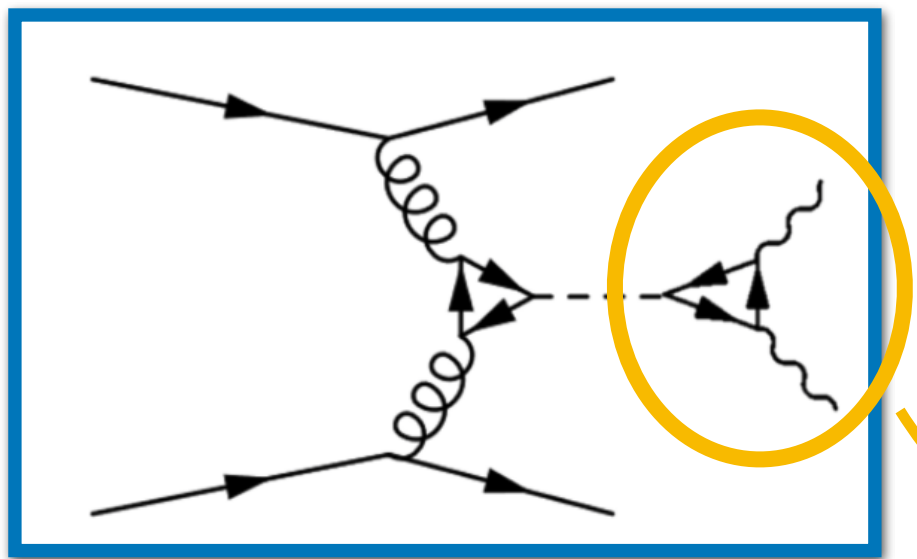


Analysis strategy

The sensitivity to the ggH anomalous coupling is indeed maximal for events with VBF-like kinematics. Therefore, making the ggH analysis orthogonal to VBF would suppress this sensitivity.

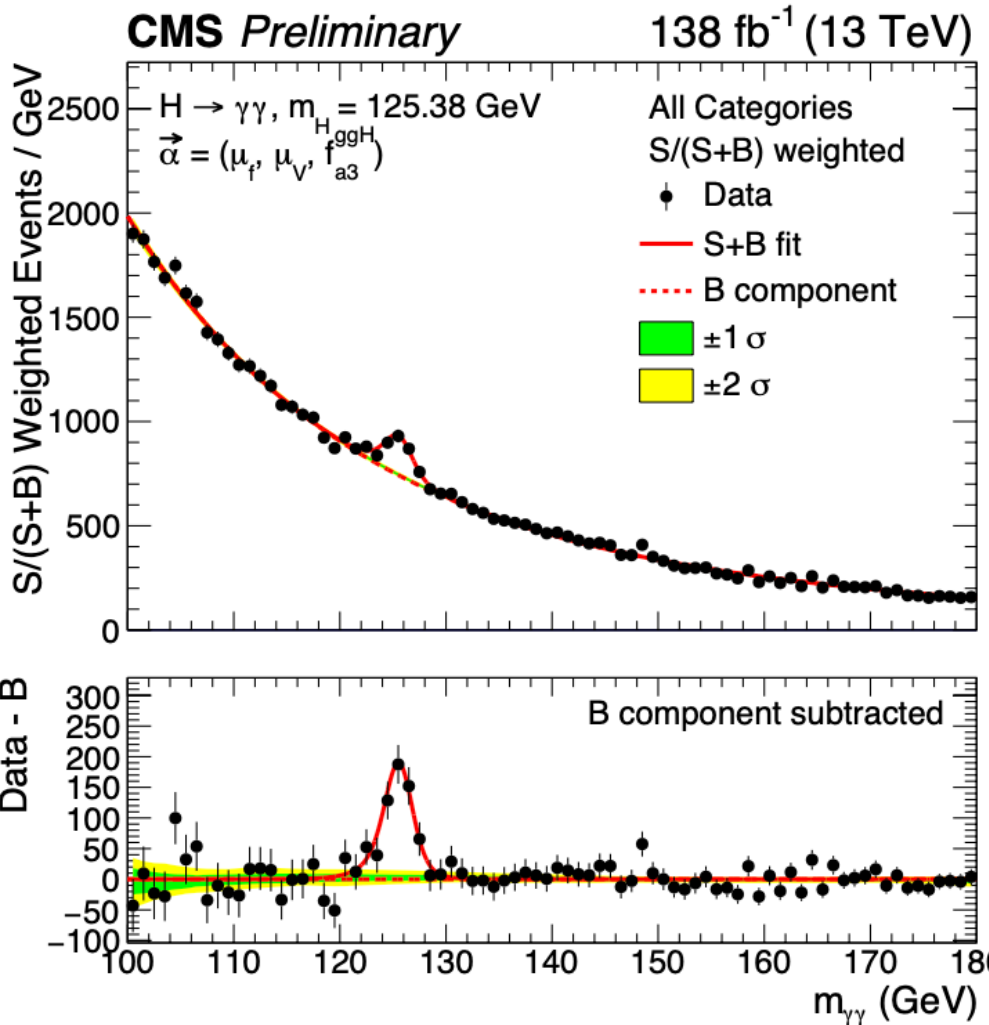


VBF ($f_{a3}, f_{a2}, f_{\Lambda_1}, f_{\Lambda_1}^{Z\gamma}$)



ggH+2Jets ($f_{a3}^{ggH}, f_{CP}^{Htt}$)

To improve clarity, from now on **pink** will be used for HVV (VBF,VH) and **blue** for the Hgg + 2 jets analysis



DATA

UL re-reco from RUN 2

NON-RESONANT BACKGROUND

estimated from Data

DIPHOTON PRESELECTION

$$|\eta_{1,2}| < 2.5, p_T/m_{\gamma\gamma} > 1/3(1/4)$$

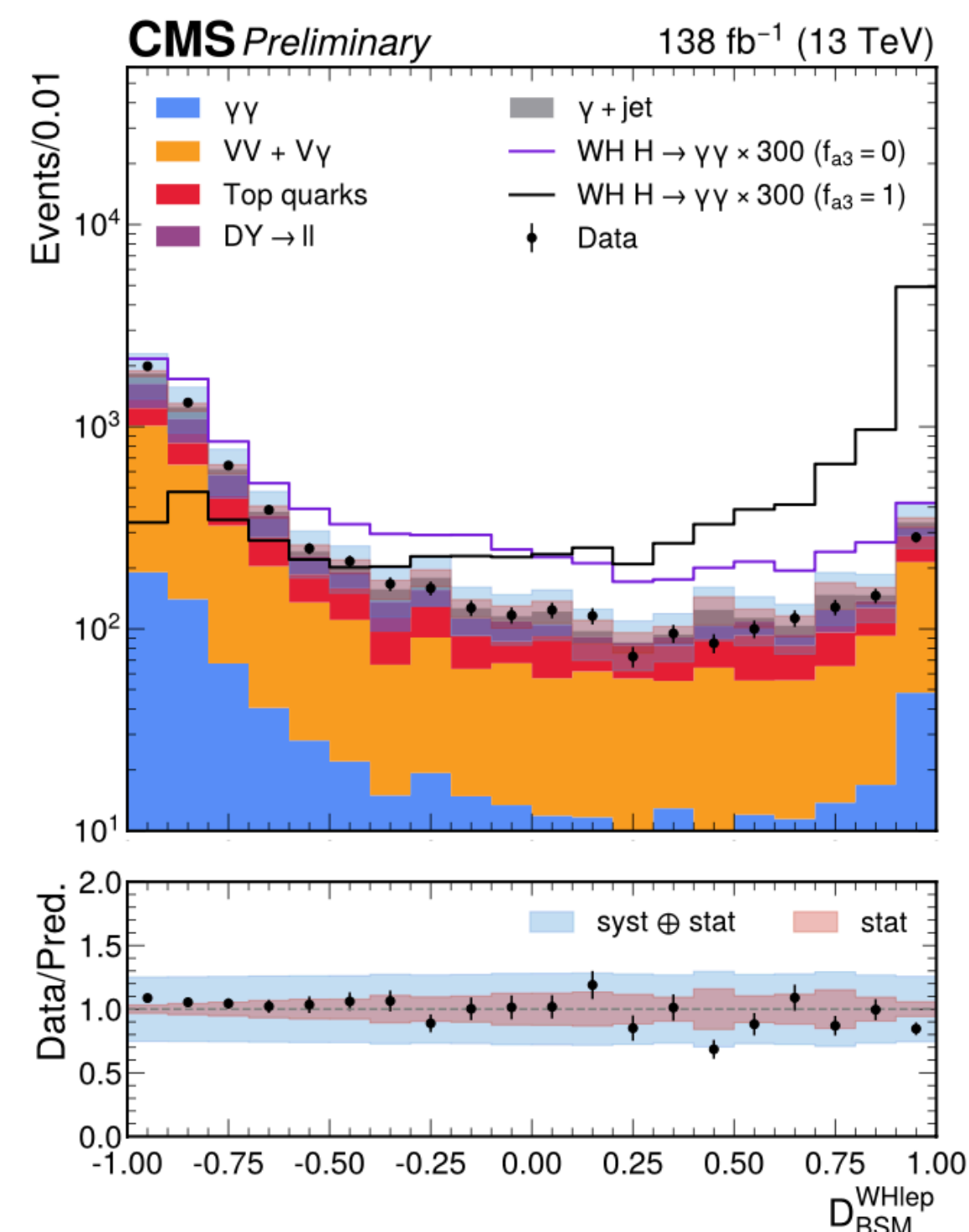
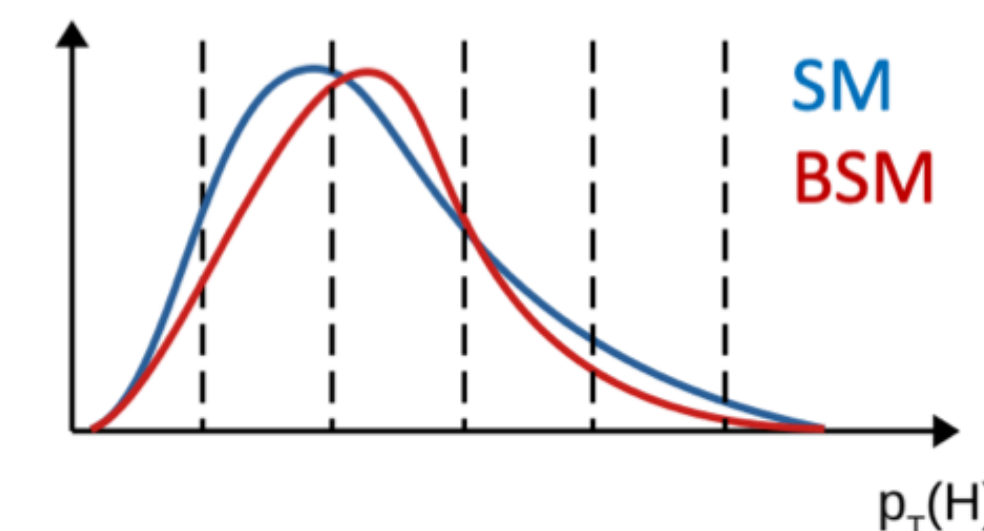
	H/E	$\sigma_{i\eta i\eta}$	R_9	Iso_{ph}	Iso_{track}
EB; $R_9 > 0.85$	< 0.08	–	–	–	–
EB; $R_9 \leq 0.85$	< 0.08	< 0.015	> 0.5	$< 4.0 \text{ GeV}$	$< 6.0 \text{ GeV}$
EE; $R_9 > 0.90$	< 0.08	–	–	–	–
EE; $R_9 \leq 0.90$	< 0.08	< 0.035	> 0.8	$< 4.0 \text{ GeV}$	$< 6.0 \text{ GeV}$
Other preselection requirements					
leading photon $p_T > 35 \text{ GeV}$	$R_9 > 0.8 \text{ OR } Iso_{ch} < 20 \text{ GeV OR } Iso_{ch}/p_T < 0.3$				
sub-leading photon $p_T > 25 \text{ GeV}$	$m_{\gamma\gamma} > 100 \text{ GeV}$				



Discriminating variables

The distributions of the kinematic variables are sensitive to Higgs quantum numbers and anomalous couplings \rightarrow CP-sensitive variables ($\Delta\phi_{jj}, p_T(H), \dots$)

MELA (Matrix Element Likelihood Approach) + **MVA** (enhance signal-to-background separation)



MVA : different strategies are applied to each production mode, according to their specific requirements

ggH+2Jets

BDT Multiclassifier

- **BKG** (non-resonant and resonant VBF)
- ggH **SM**
- ggH **BSM** (CP-odd)

VBF and VH-had

Two **DNN** for the two prediction modes

- **BKG** (resonant and non-resonant background)
- VBF/VH-had **SM**
- VBF/VH-had **BSM** (CP-odd)

VH-lep

Separate with 2 **BDT**

- **STXS BDT** score (to separate BKG and VH-lep SM)
- **AC BDT** score (to separate VH-lep BSM and VH-lep SM)

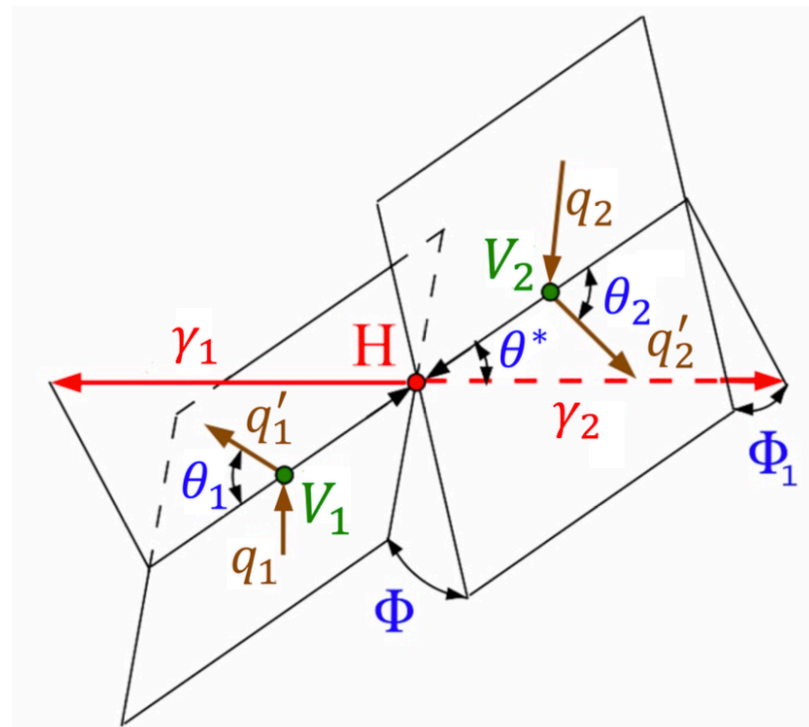


Discriminating variables

MELA (Matrix Element Likelihood Approach) : For ggH, VBF, VH we can define a set of 7 observables (Ω^{prod}) that fully describe the topology

$$\Omega^{prod} = \{\theta_1^{prod}, \theta_2^{prod}, \theta^{*prod}, \Phi^{prod}, \Phi_1^{prod}, p_1^{2,Vprod}, p_2^{2,prod}\} \quad (\text{where } prod = \text{VBF, VH, ggH})$$

The method is designed to reduce the number of observables to a minimum, while retaining all important information



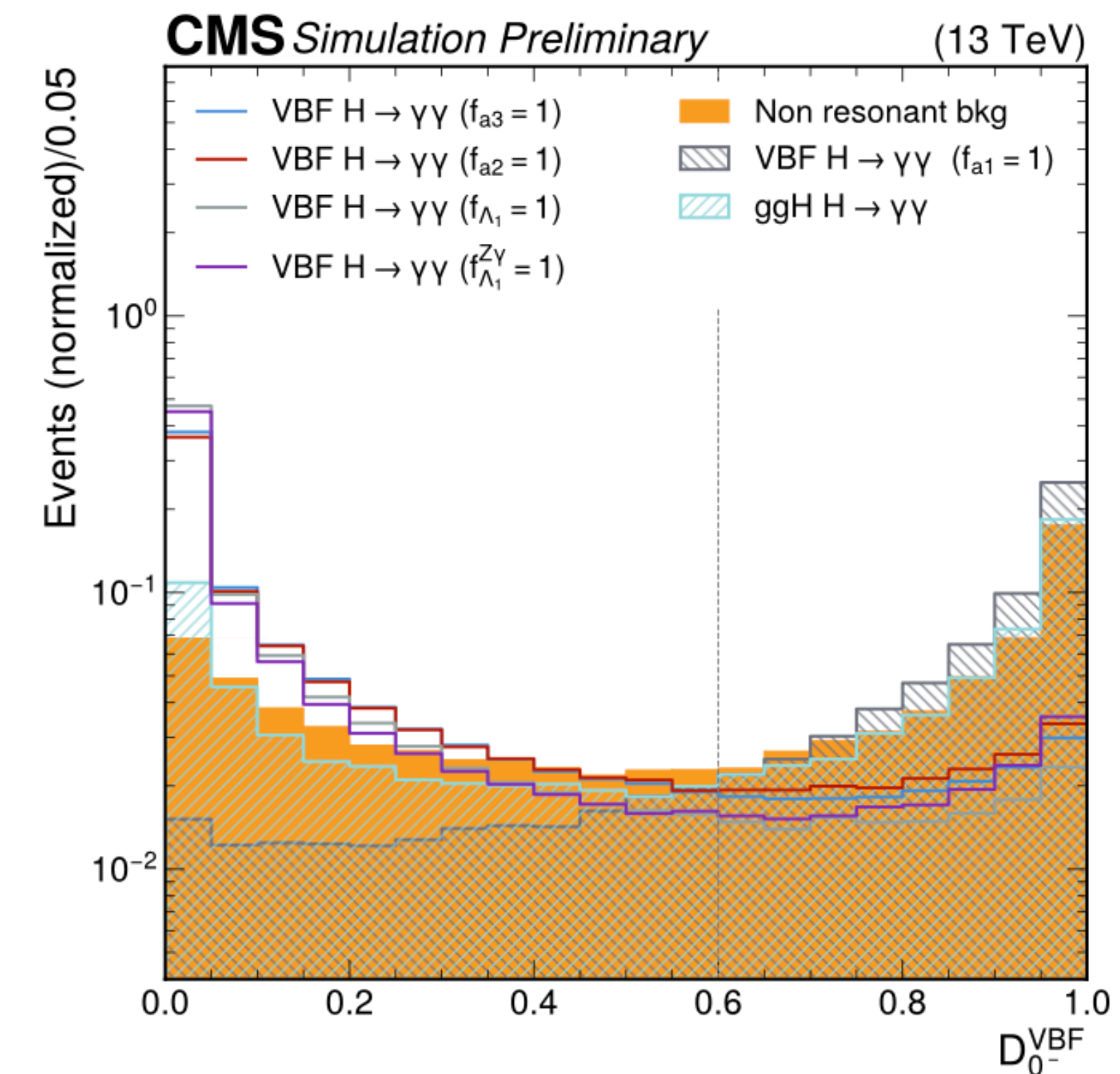
$$\mathcal{D}_{BSM} = \frac{\mathcal{P}_{SM}(\vec{\Omega})}{\mathcal{P}_{SM}(\vec{\Omega}) + \mathcal{P}_{BSM}(\vec{\Omega})}$$

Separate SM and BSM couplings

$$\mathcal{D}_{int} = \frac{\mathcal{P}_{SM-BSM}^{int}(\vec{\Omega})}{\mathcal{P}_{SM}(\vec{\Omega}) + \mathcal{P}_{BSM}(\vec{\Omega})}$$

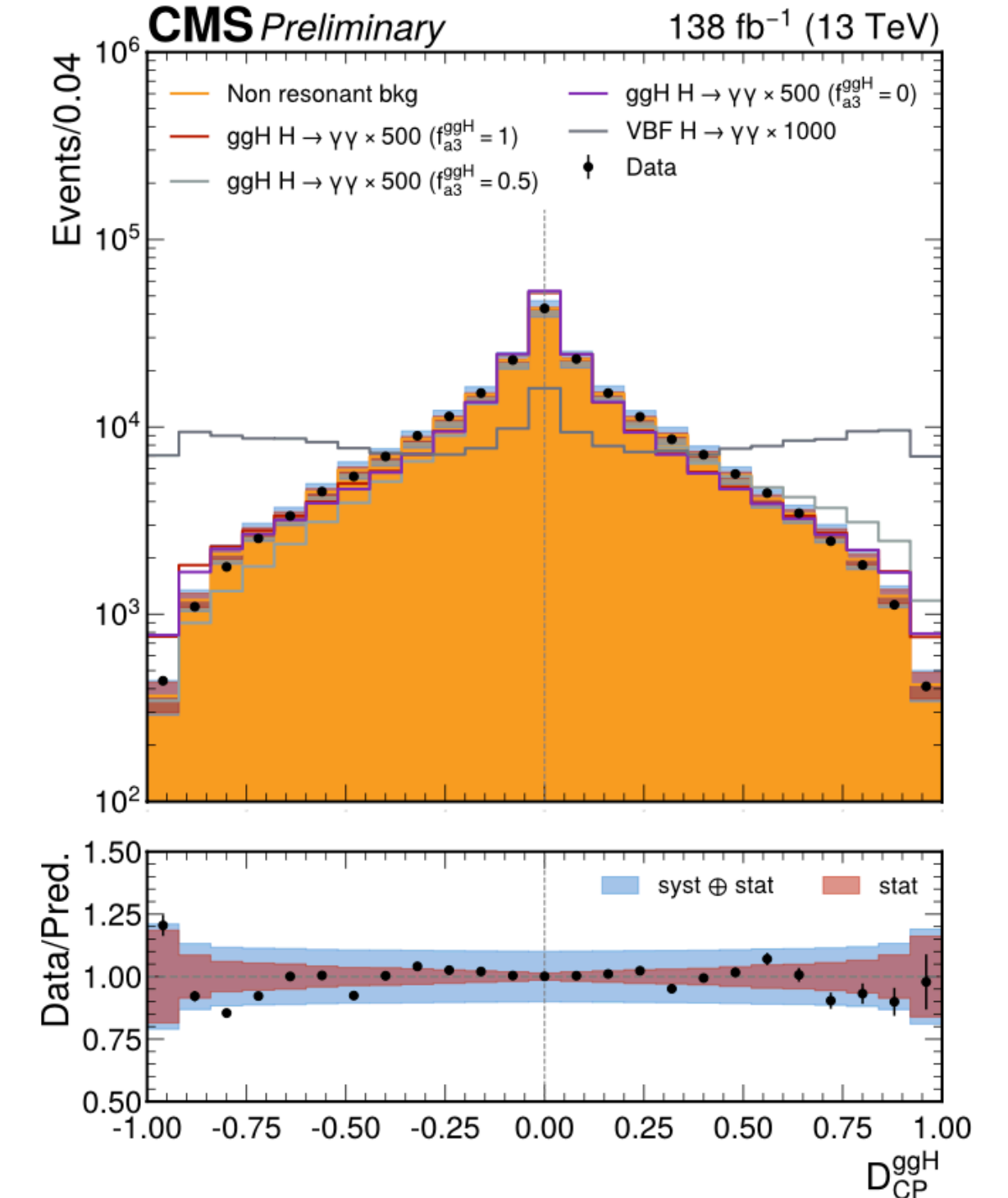
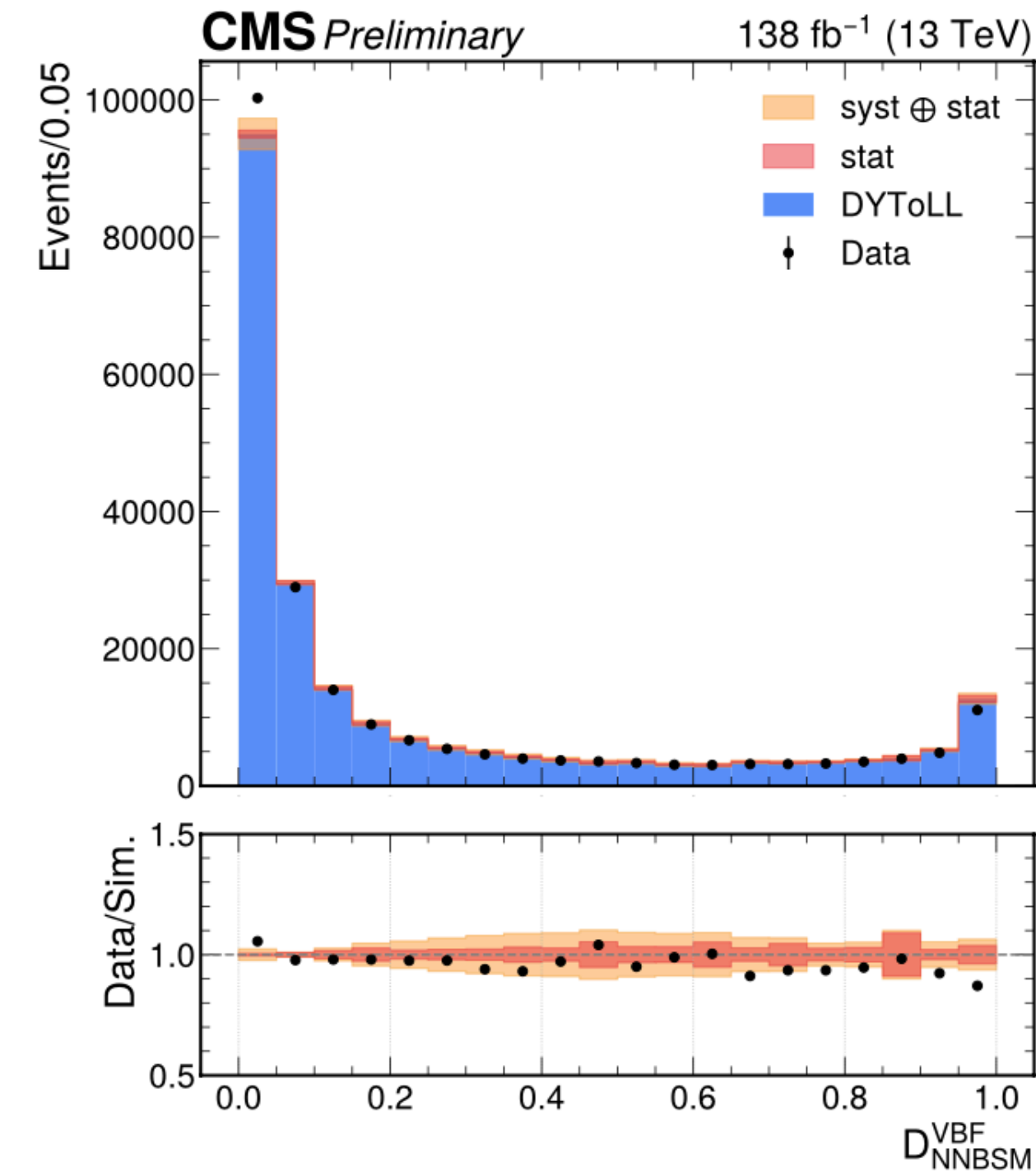
Sensitive to interference between SM and BSM couplings

D_{0-}^{VBF} is designed to distinguish between CP-even and CP-odd scenarios, but it also performs well for other anomalous coupling scenarios ($a_2, \Lambda_1, \Lambda_1^{Z\gamma}$). **Therefore, the same categorization is applied to target all anomalous couplings.**



Validation

Production mode	Discr.	Goal
ggH	\mathcal{D}_{0-}^{ggH}	CP -even VS CP -odd scenarios
ggH	\mathcal{D}_{CP}^{ggH}	Probe the interference
ggH	\mathcal{D}_{STXS}^{ggH}	Higgs signal VS non-resonant background
ggH	$\mathcal{D}_{bkg}^{ggH+2jets}$	ggH + 2 jets (SM and CP -odd) VS rest
ggH	$\mathcal{D}_{BSM}^{ggH+2jets}$	ggH + 2 jets (CP -odd) VS rest
VBF	\mathcal{D}_{0-}^{VBF}	SM VS CP -odd scenarios
VBF	$\mathcal{D}_{NNbkg}^{VBF}$	Higgs signal VS non-resonant background
VBF	$\mathcal{D}_{NNBSM}^{VBF}$	SM Higgs VS BSM Higgs
VH-hadronic	\mathcal{D}_{bkg}^{had}	Higgs signal VS non-resonant background
VH-hadronic	\mathcal{D}_{BSM}^{had}	SM Higgs VS BSM Higgs
$W(\ell\nu)$ -leptonic	\mathcal{D}_{STXS}^{lep}	Higgs signal VS non-resonant background
$W(\ell\nu)$ -leptonic	\mathcal{D}_{BSM}^{lep}	SM Higgs VS BSM Higgs
$Z(\ell\ell)$ -leptonic	\mathcal{D}_{STXS}^{lep}	Higgs signal VS non-resonant background
$Z(\ell\ell)$ -leptonic	\mathcal{D}_{BSM}^{lep}	SM Higgs VS BSM Higgs
$Z(\nu\nu)$ -MET	\mathcal{D}_{STXS}^{MET}	Higgs signal VS non-resonant background
$Z(\nu\nu)$ -MET	\mathcal{D}_{BSM}^{MET}	SM Higgs VS BSM Higgs

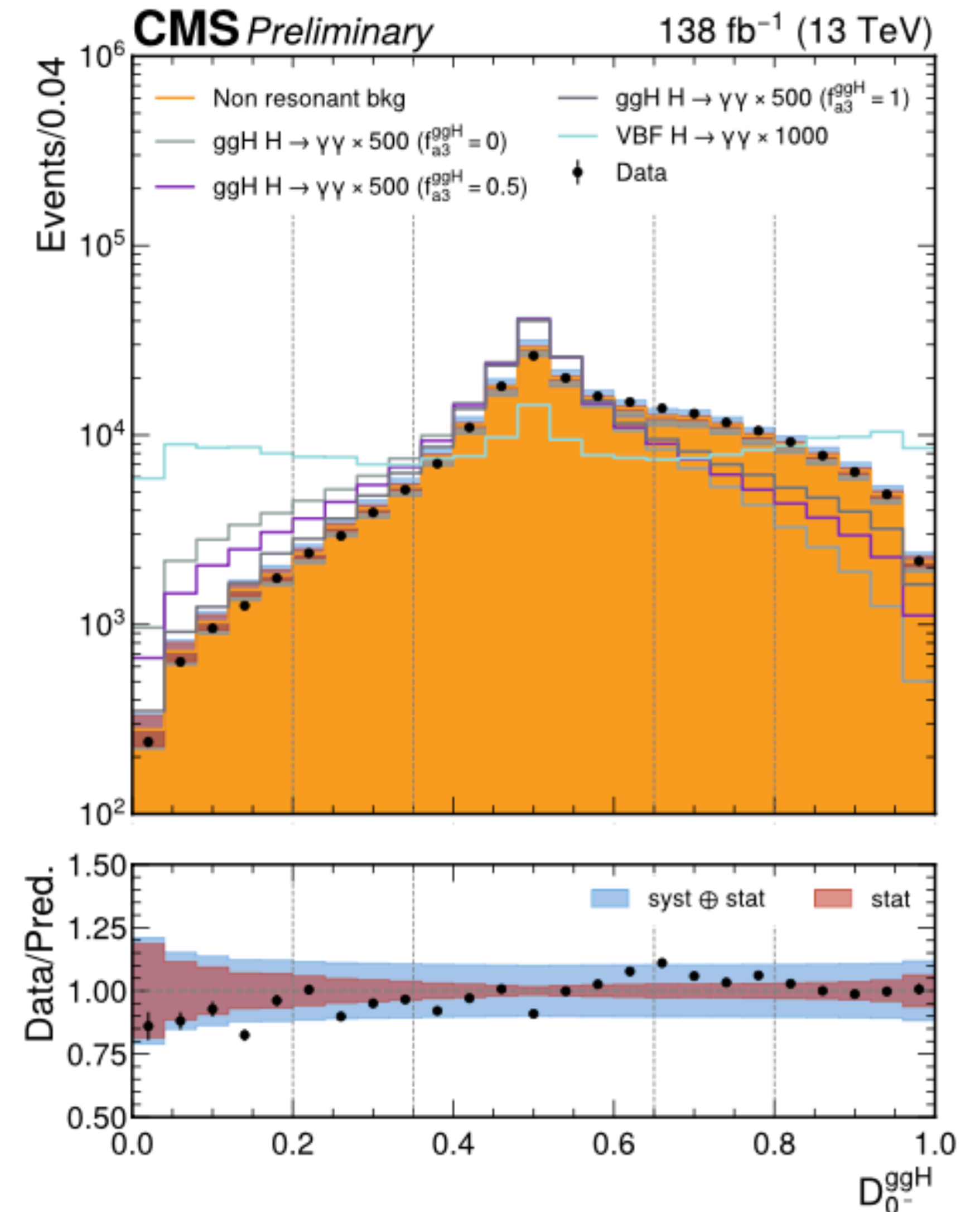


The output of the MVA variables has been validated using a sample of $Z \rightarrow ee$ events (where both electrons are reconstructed as photons) and non resonant background events. A **good agreement between data and Monte Carlo** simulation is observed, confirming the robustness of the modeling

Categories optimization (Hgg)

Three-dimensional categorization ($D_{0^-}^{ggH}, D_{STXS}^{ggH}, D_{CP}^{ggH}$) in **30 bins** based on:

- ▶ **5 bins** in **MELA variable** $D_{0^-}^{ggH}$ to separate SM and BSM states
- ▶ **3 bins** in **standard di-photon MVA** (D_{STXS}^{ggH}) to reduce continuum background
- ▶ **2 bins** in **MELA variable** D_{CP}^{ggH} to be sensitive to the sign of the interference term



Categories optimization (HVV)

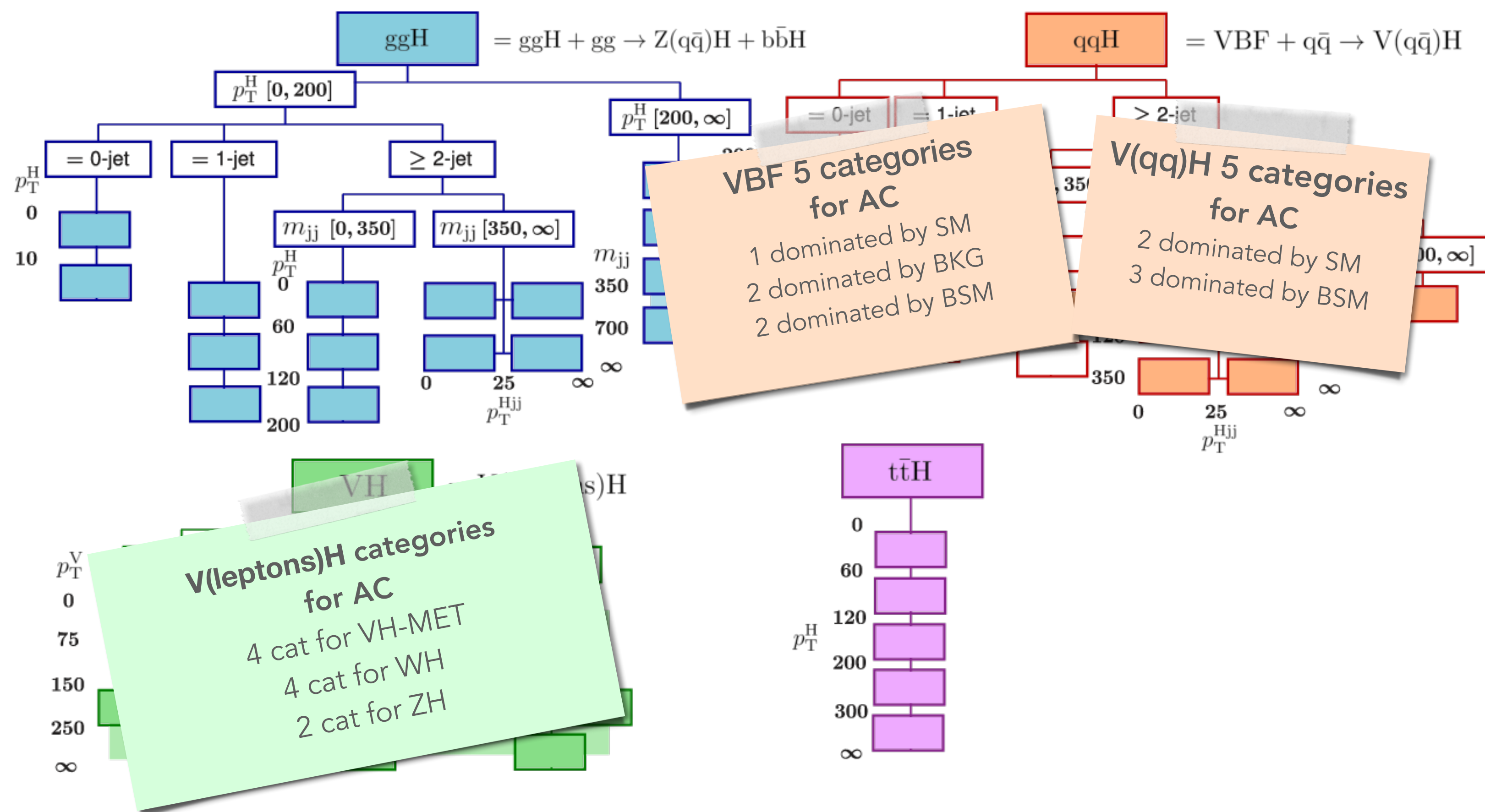
This analysis targets the HVV couplings, whose sensitivity comes from either the VBF, or the associated productions of WH and ZH.

For both the VBF and VH associated production, the phase space used is the same

of the Run2 STXS analysis [[HIG-19-015](#)]

→ (STXS AN (i.e. $\mu_{ggH}, \mu_{VBF}, \mu_{VH}, \mu_{top}$))

Create categories in the discriminant phase space such that they maximize signal significance while maintaining a minimum number of data sideband events

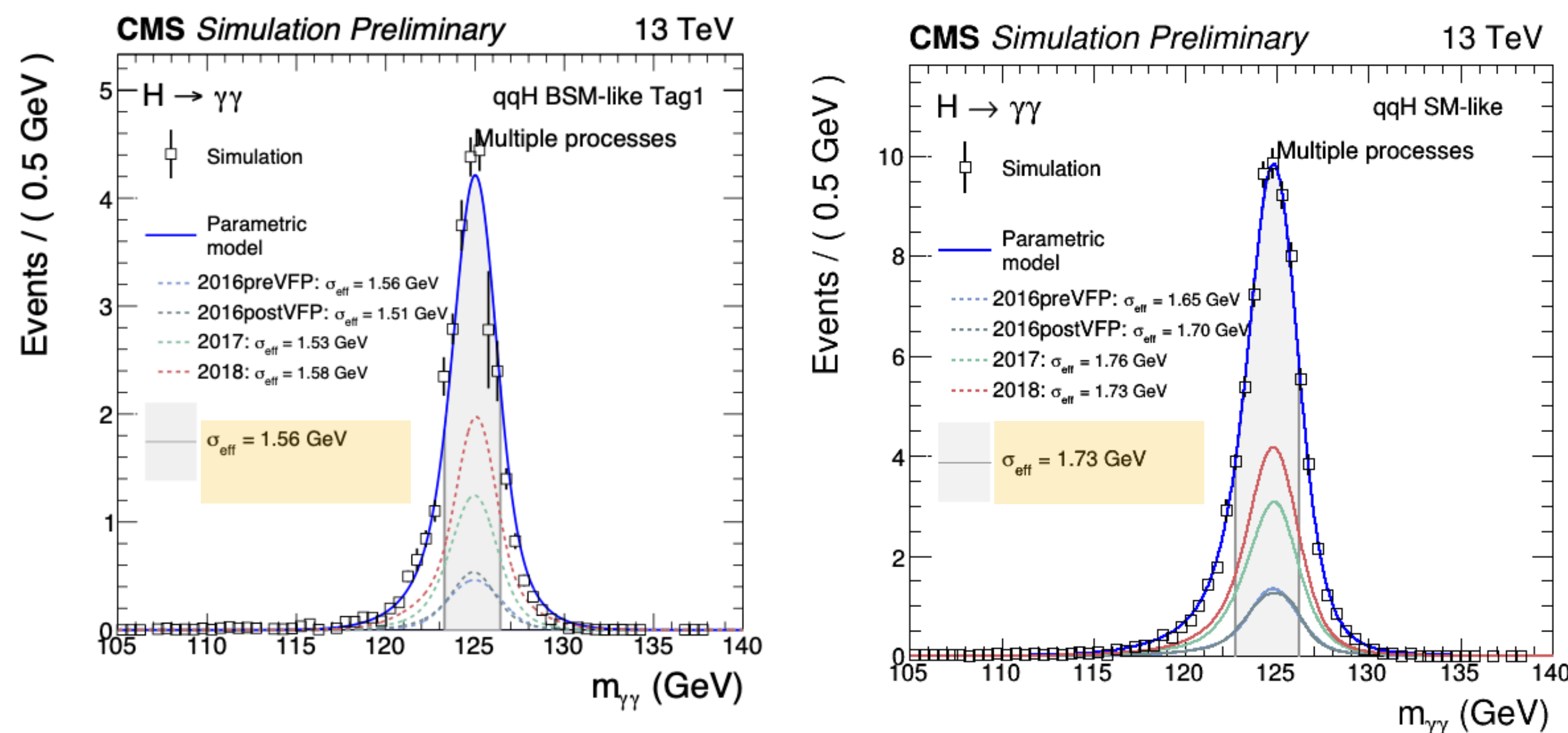


Signal and Background modeling

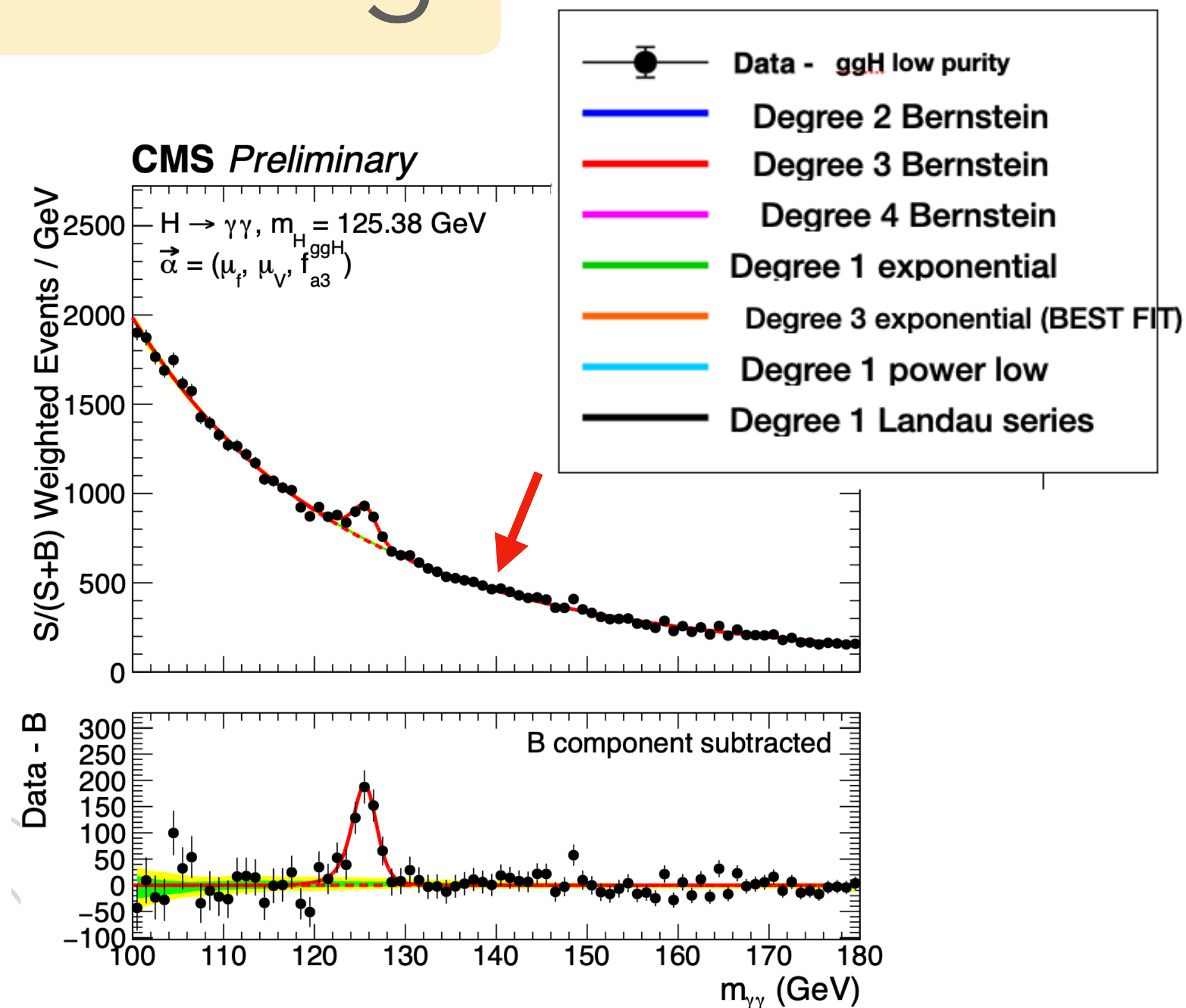
Typical procedure used in all $H \rightarrow \gamma\gamma$ analyses

the procedure applies to both **HVV** and **ggH** analyses

Fit each (year x prod. modes x category x vertex-scenario) separately and determine **optimum number of Gaussians**



*When the interaction point is known with a precision worse than 1 cm, the resolution on the photon opening angle becomes a non-negligible contribution to the mass resolution



discrete profiling method: the choice of background function is treated as a systematic uncertainty

Fit strategy

- Binned maximum likelihood uses in the fit:

PROBABILITY DENSITY FUNCTION

$$P_k(m_{\gamma\gamma}; \vec{\theta}_k, \vec{\mu}, f_i) = \sum_j \mu_j P_{jk}^{sig}(m_{\gamma\gamma}; \vec{\theta}_{jk}, f_i) + P_k^{bkg}(m_{\gamma\gamma}; \vec{\theta}_k)$$

INTERFERENCE

$$P_{jk}^{sig}(m_{\gamma\gamma}; \vec{\theta}_{jk}, f_i) = (1 - f_i) P_{jk}^{a_1}(m_{\gamma\gamma}; \vec{\theta}_{jk}) + f_i P_{jk}^i(m_{\gamma\gamma}; \vec{\theta}_{jk}) - 2\sqrt{f_i(1 - f_i)} \cos(\phi_{ai}) P_{jk}^{a_1, a_i}(m_{\gamma\gamma}; \vec{\theta}_{jk})$$

- * j = process (VBF, VH, TT, GGH)
- * k = category

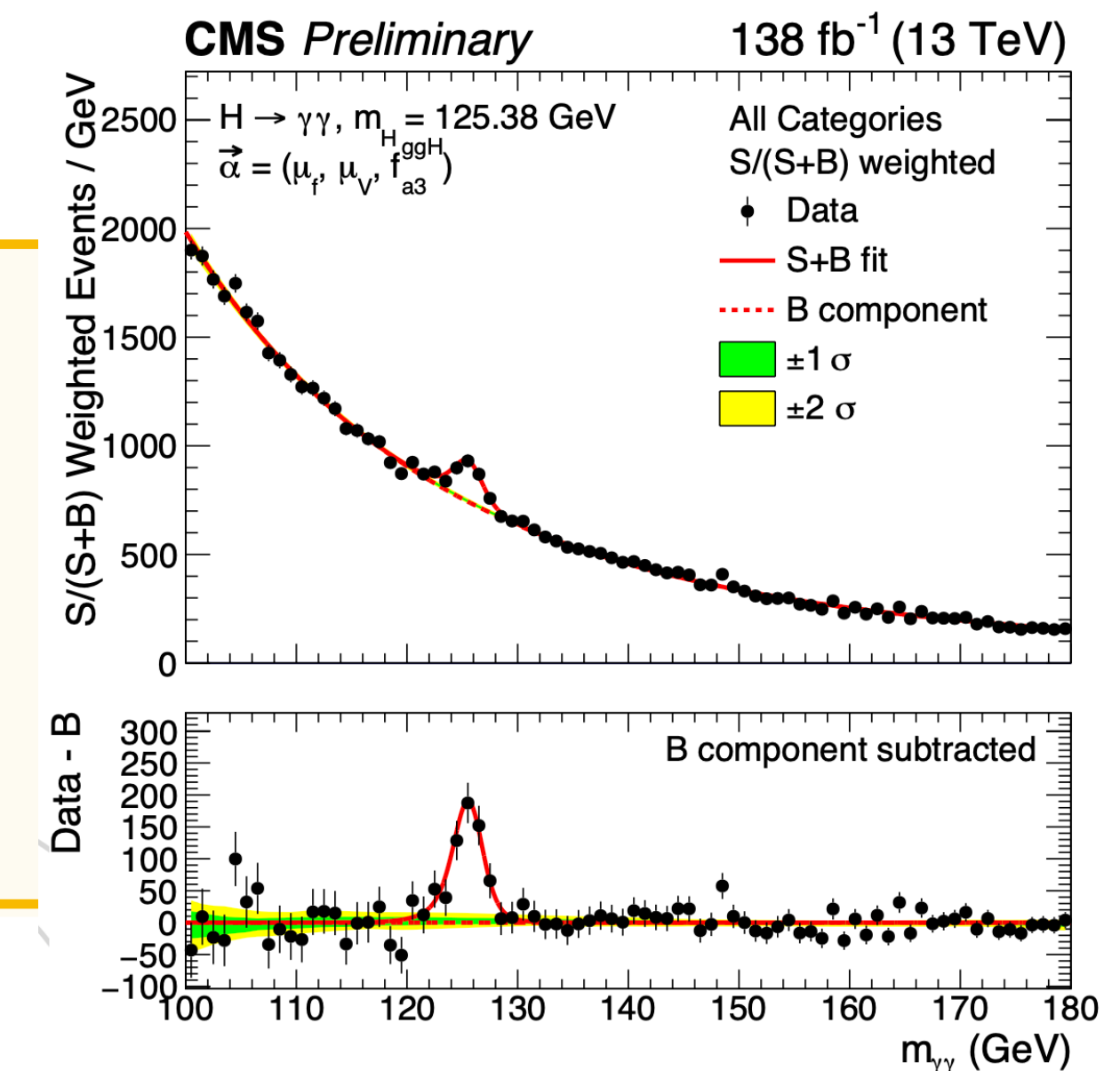
PARAMETERS OF INTEREST: signal strength per process ($\mu_j = \mu_V, \mu_f$) + anomalous cross section fraction (f_{ai}): **two independent fits are done for HVV and Hgg**

HVV : f_{ai} ($f_{a3}, f_{a2}, f_{\Lambda 1}, f_{\Lambda 1}^{Z\gamma}$) fitted and μ_V, μ_f are floating

ggH : f_{a3}^{ggH} is fitted and μ_f, μ_V are floating

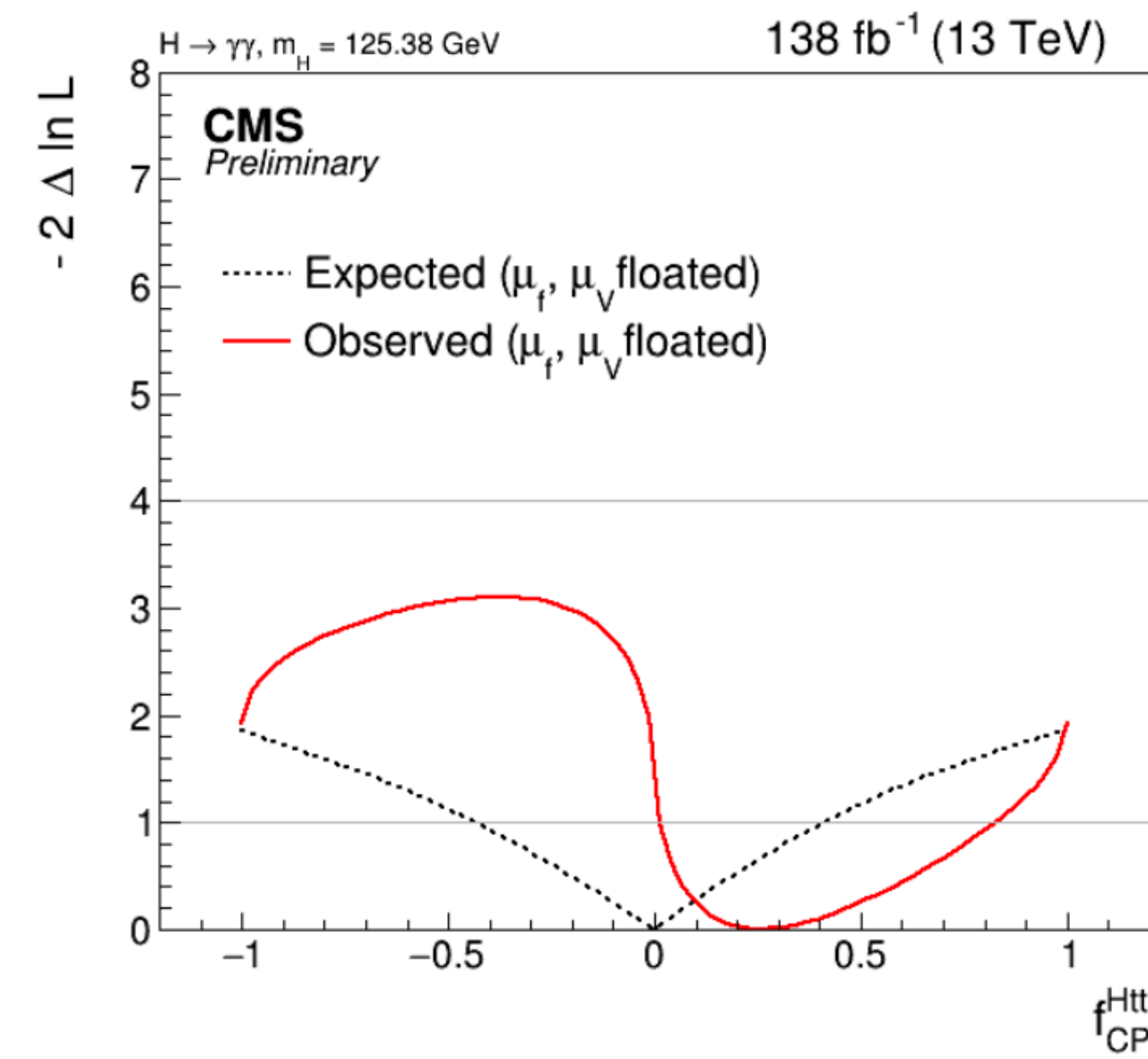
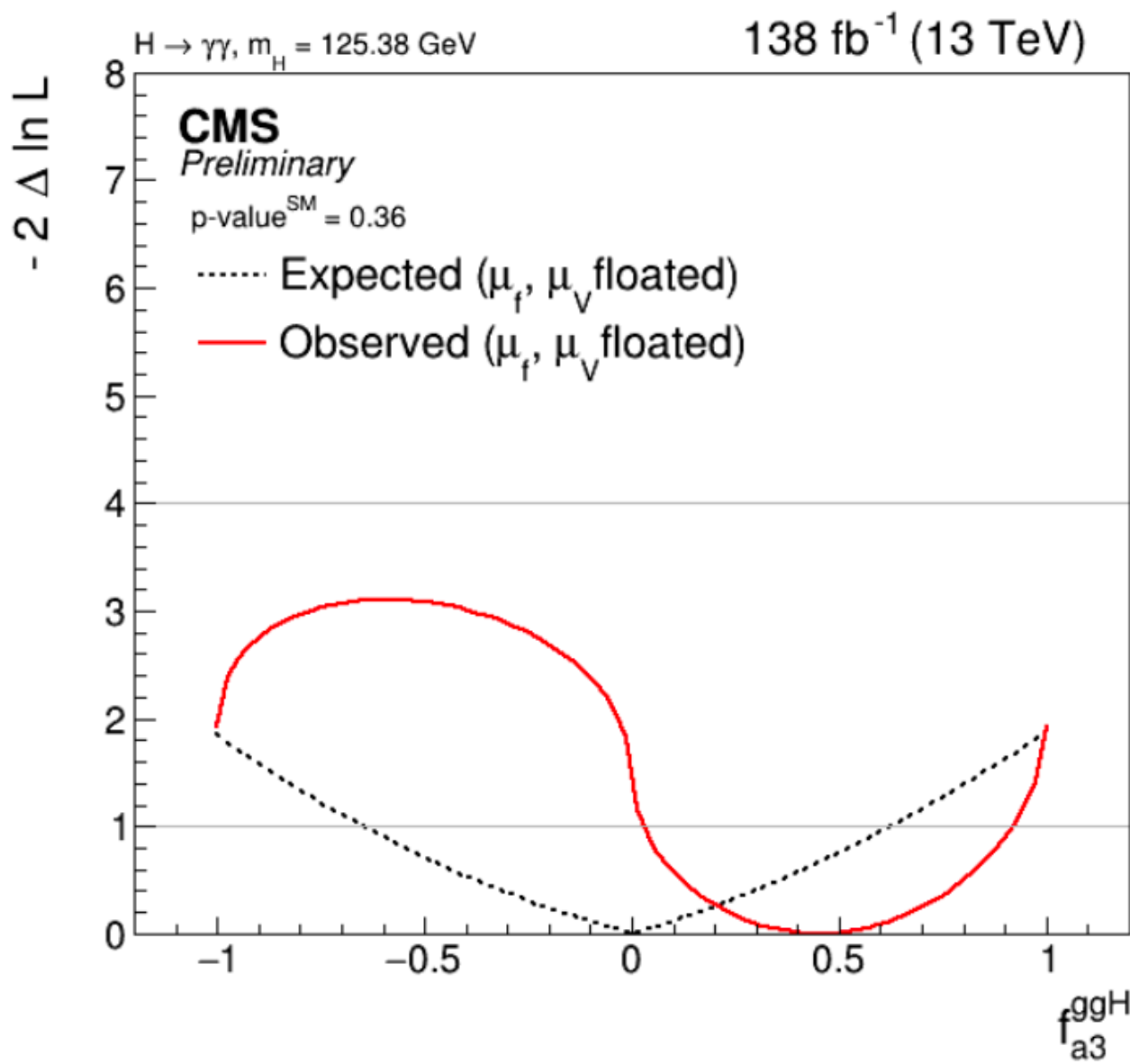
NUISANCE

The systematic uncertainties have a limited impact, contributing less than 10% to the total uncertainty.

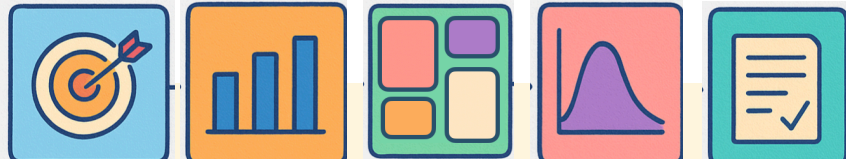


Likelihood scan (Hgg)

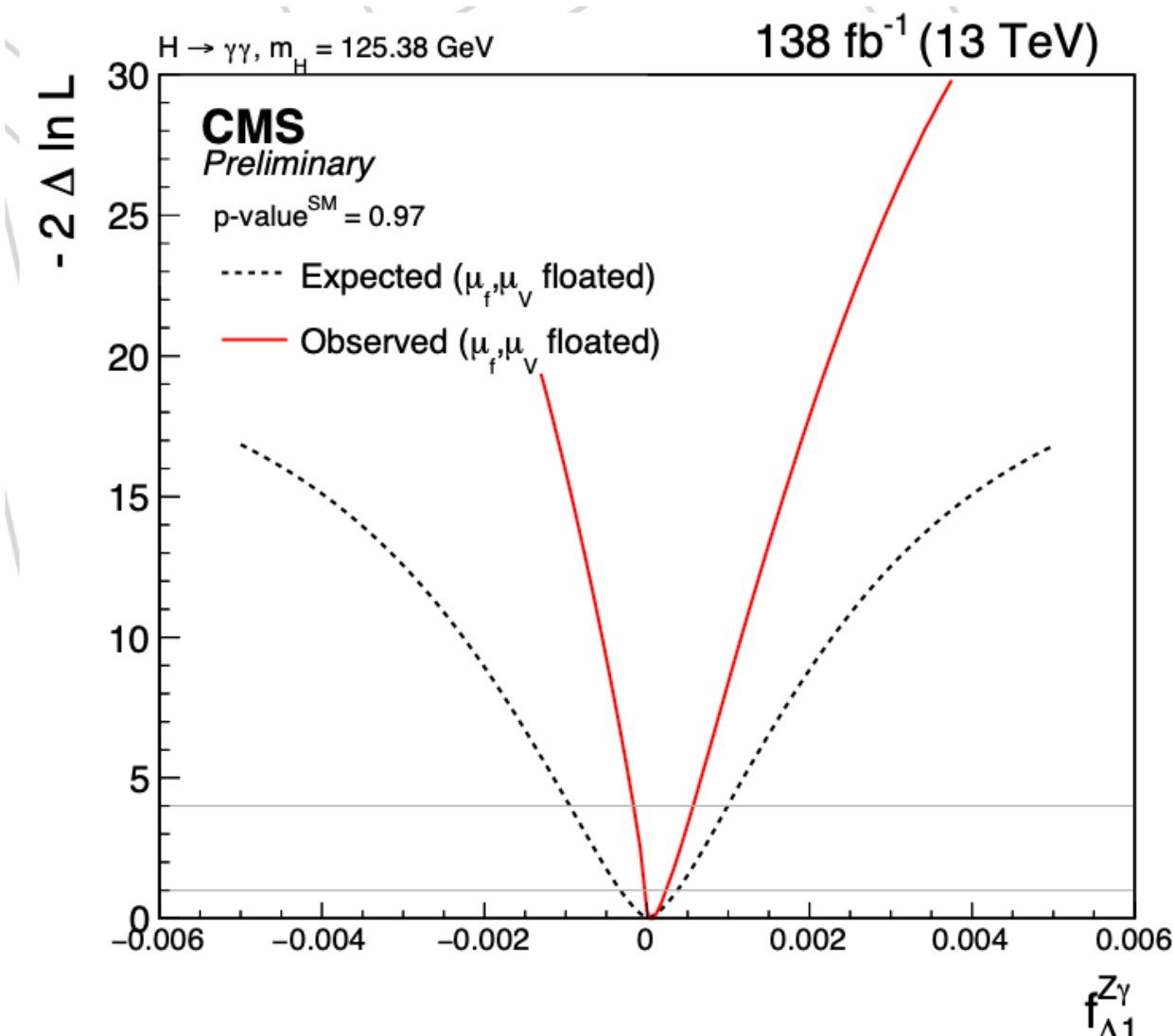
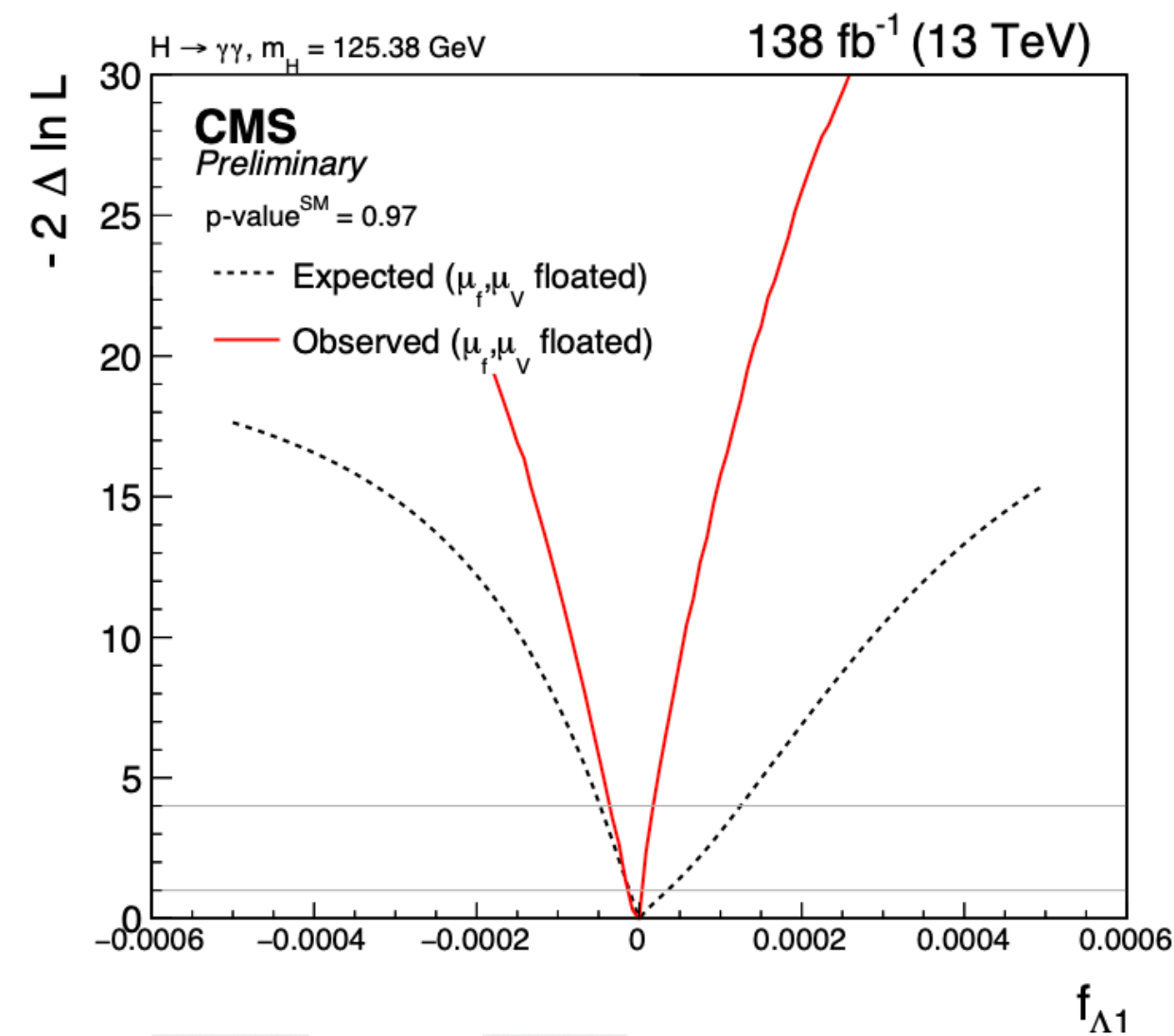
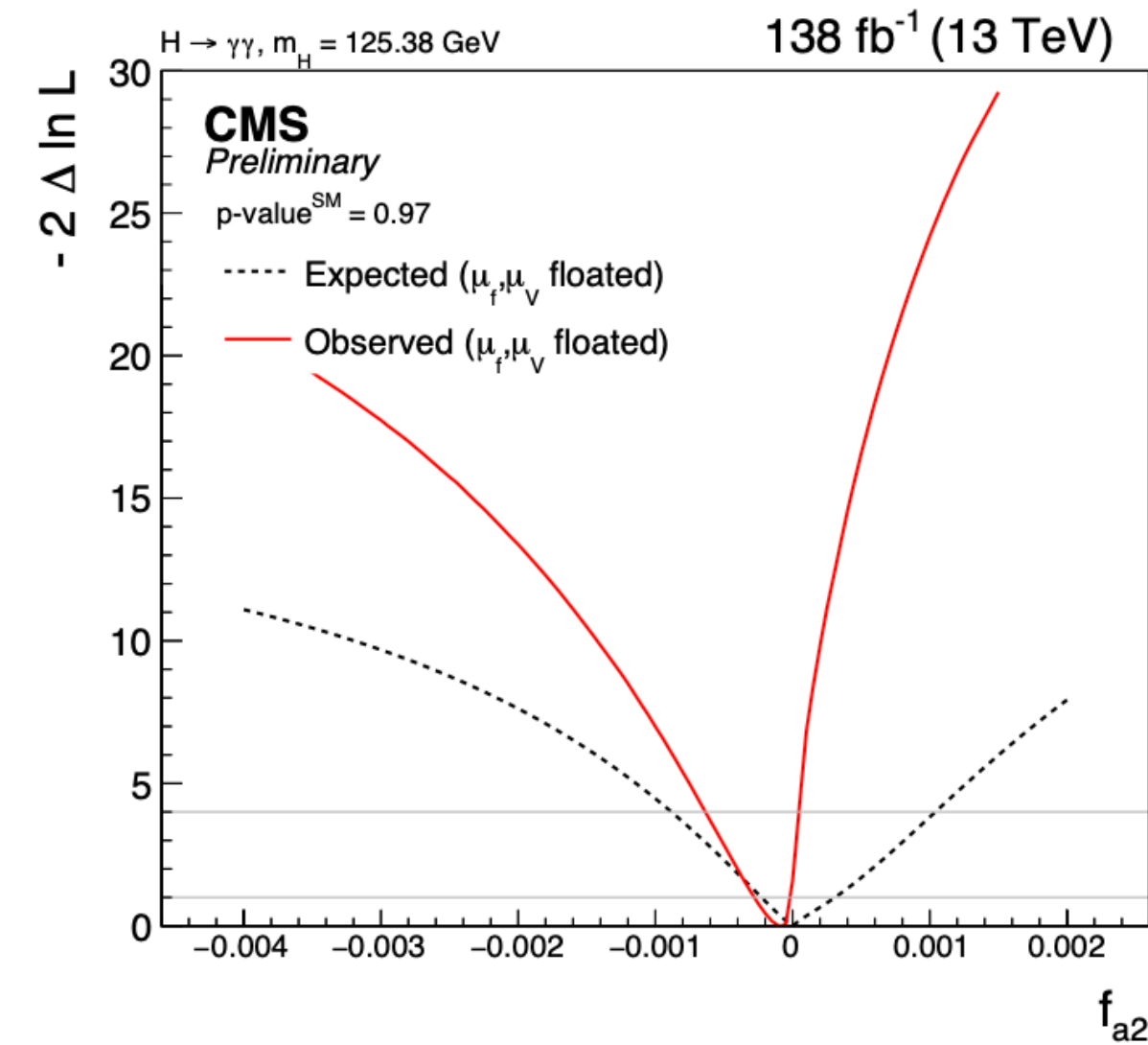
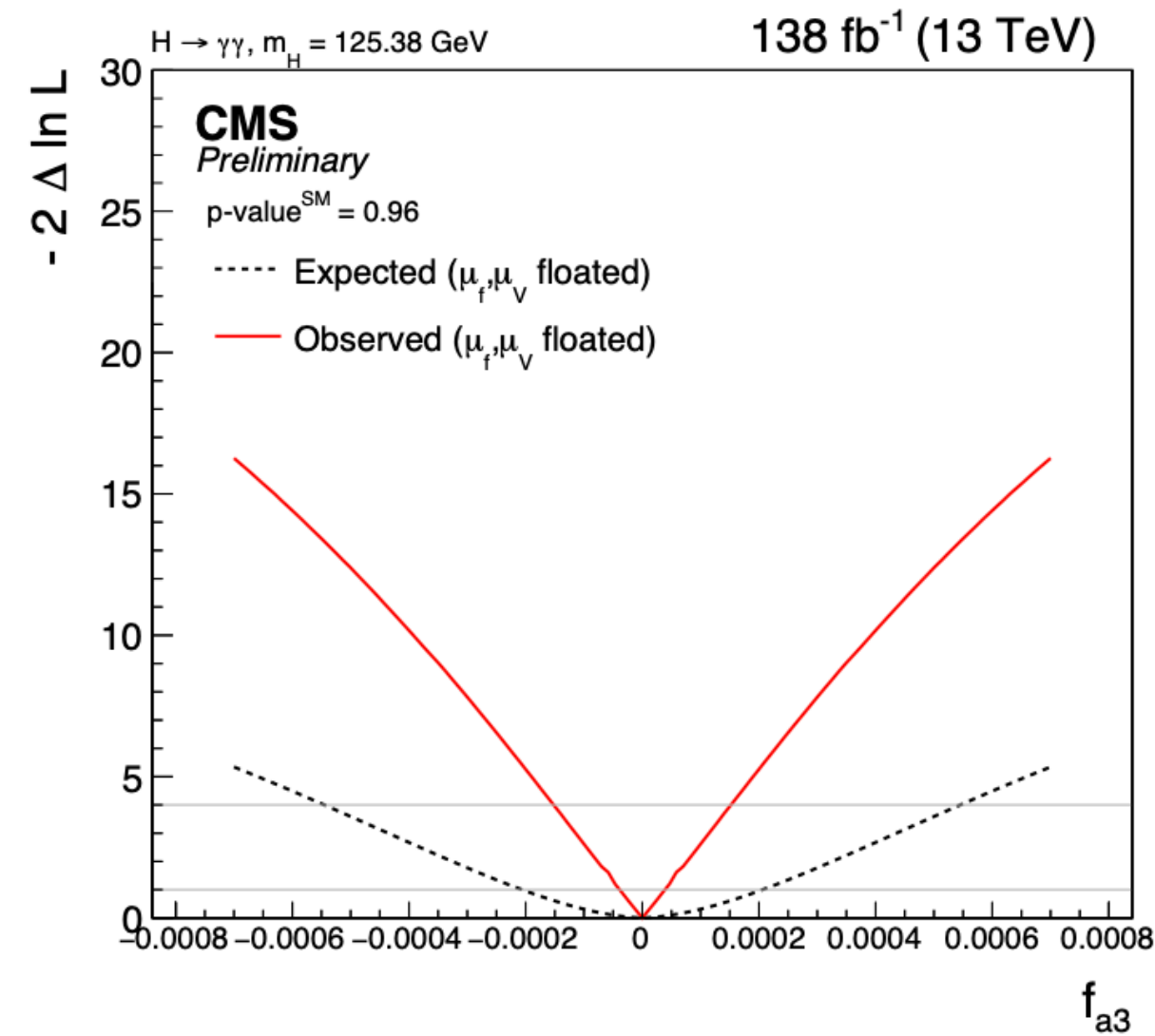
- Compatible wrt SM prediction ($f_{ai} = 0$)
- Comparable limits wrt previous measurement



Parameter	Scenario	Observed		Expected	
		68% C.L.	95% C.L.	68% C.L.	95% C.L.
f_{a3}^{ggH}	ggH (4ℓ)	$-0.04^{+1.04}_{-0.96}$	$[-1, 1]$	0 ± 1	$[-1, 1]$
	ggH ($\tau\tau$)	$0.07^{+0.32}_{-0.07}$	$[-0.15, 0.89]$	0.00 ± 0.26	$[-1, 1]$
	ggH (W W)	$0.03^{+0.72}_{-0.38}$	$[-1, 1]$	$[-1, 1]$	$[-1, 1]$
	ggH ($\gamma\gamma$)	$0.45^{+0.47}_{-0.43}$	$[-1, 1]$	$0.00^{+0.63}_{-0.65}$	$[-1, 1]$
f_{CP}^{Htt}	tH, $t\bar{t}H$ (4ℓ)	$\pm(0.88^{+0.12}_{-1.88})$	$[-1, 1]$	0 ± 1	$[-1, 1]$
	tH, $t\bar{t}H$ ($\gamma\gamma$)	0.00 ± 0.33	$[-0.67, 0.67]$	0.00 ± 0.49	$[-0.82, 0.82]$
	tH, $t\bar{t}H$ ($4\ell, \gamma\gamma$)	0.00 ± 0.33	$[-0.67, 0.67]$	0.00 ± 0.48	$[-0.81, 0.81]$
	ggH (4ℓ)	$-0.01^{+1.01}_{-0.99}$	$[-1, 1]$	0 ± 1	$[-1, 1]$
	ggH ($\tau\tau$)	$0.03^{+0.17}_{-0.03}$	$[-0.07, 0.51]$	0.00 ± 0.12	$[-0.49, 0.49]$
	ggH, tH, $t\bar{t}H$ (4ℓ)	$-0.56^{+1.56}_{-0.44}$	$[-1, 1]$	0.00 ± 0.47	$[-1, 1]$
	ggH, tH, $t\bar{t}H$ ($4\ell, \gamma\gamma$)	$-0.04^{+0.38}_{-0.36}$	$[-0.69, 0.68]$	0.00 ± 0.30	$[-0.70, 0.70]$
	ggH ($\gamma\gamma$)	$0.26^{+0.57}_{-0.25}$	$[-1, 1]$	$0.00^{+0.41}_{-0.43}$	$[-1, 1]$



Likelihood scan (HVV)



Parameter	Expected/(10 ⁻⁴) $H \rightarrow \gamma\gamma$ (68% CL)	Observed/(10 ⁻⁴) $H \rightarrow \gamma\gamma$ (68% CL)	Expected/(10 ⁻⁴) $H \rightarrow 4\ell + H \rightarrow \tau^+\tau^-$ (68% CL)
f_{a3}	$0.0^{+2.1}_{-2.1}$	$0.00^{+0.39}_{-0.39}$	$[-0.5, 0.5]$
f_{a2}	$0.0^{+3.1}_{-2.3}$	$-0.81^{+0.65}_{-2.0}$	$[-4, 5]$
$f_{\Lambda 1}$	$0.0^{+0.35}_{-0.12}$	$-0.014^{+0.032}_{-0.14}$	$[-0.4, 1.1]$
$f_{\Lambda 1}^{Z\gamma}$	$0.0^{+3.7}_{-3.3}$	$0.83^{+1.5}_{-0.92}$	$[-10, 10]$

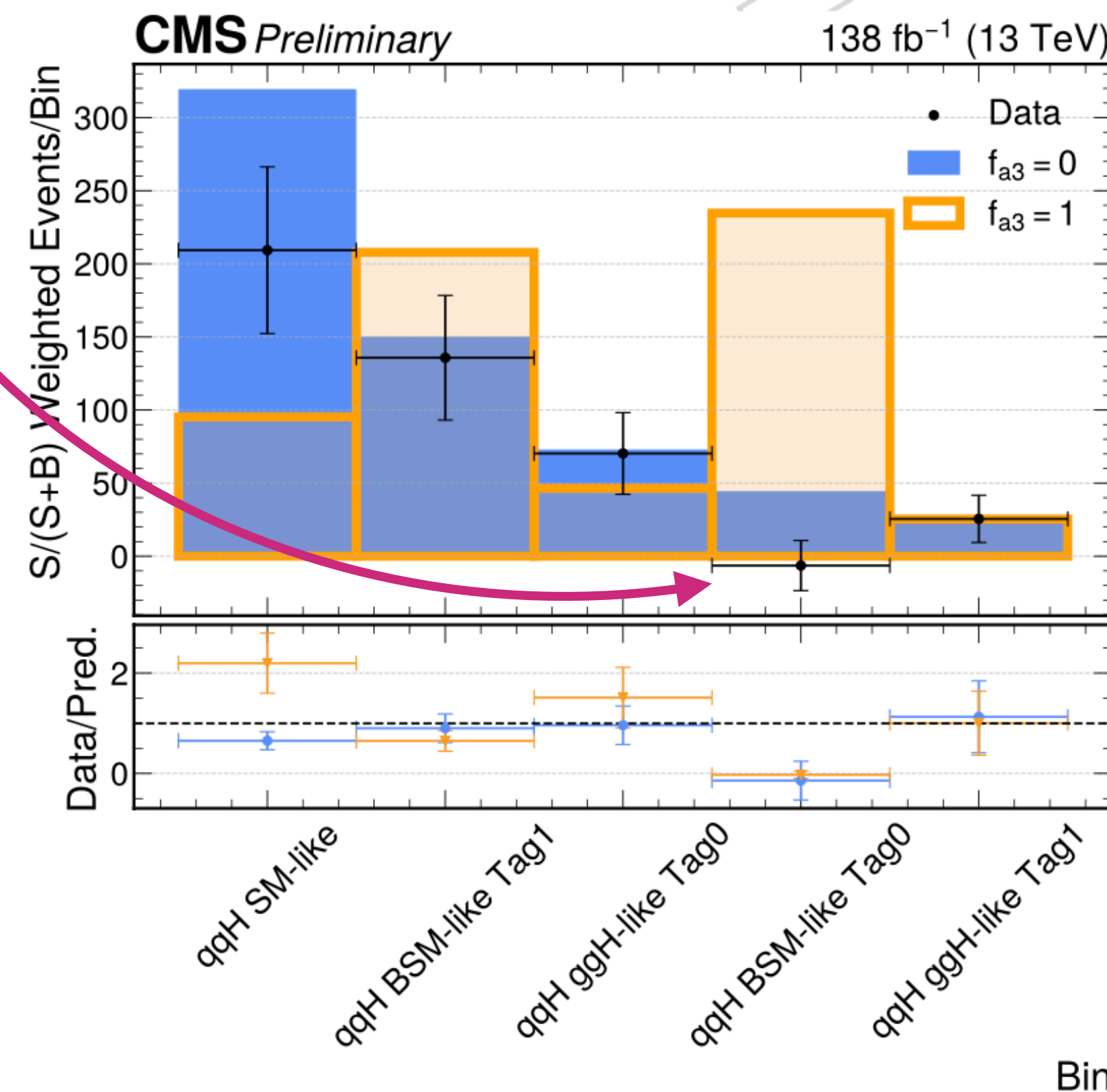
only one f_{ai} ($f_{a3}, f_{a2}, f_{\Lambda 1}, f_{\Lambda 1}^{Z\gamma}$) is fitted at a time while μ_V, μ_f are floating



RESULTS

Observed yields

As shown by the results, the observed curve reaches a higher sensitivity than expected. This can be attributed to two main factors: first, the fitted value of μ_V is higher than expected ($\mu_V \sim 1.37$); second the categories with the highest sensitivity exhibit an **under-fluctuation** in the observed data,

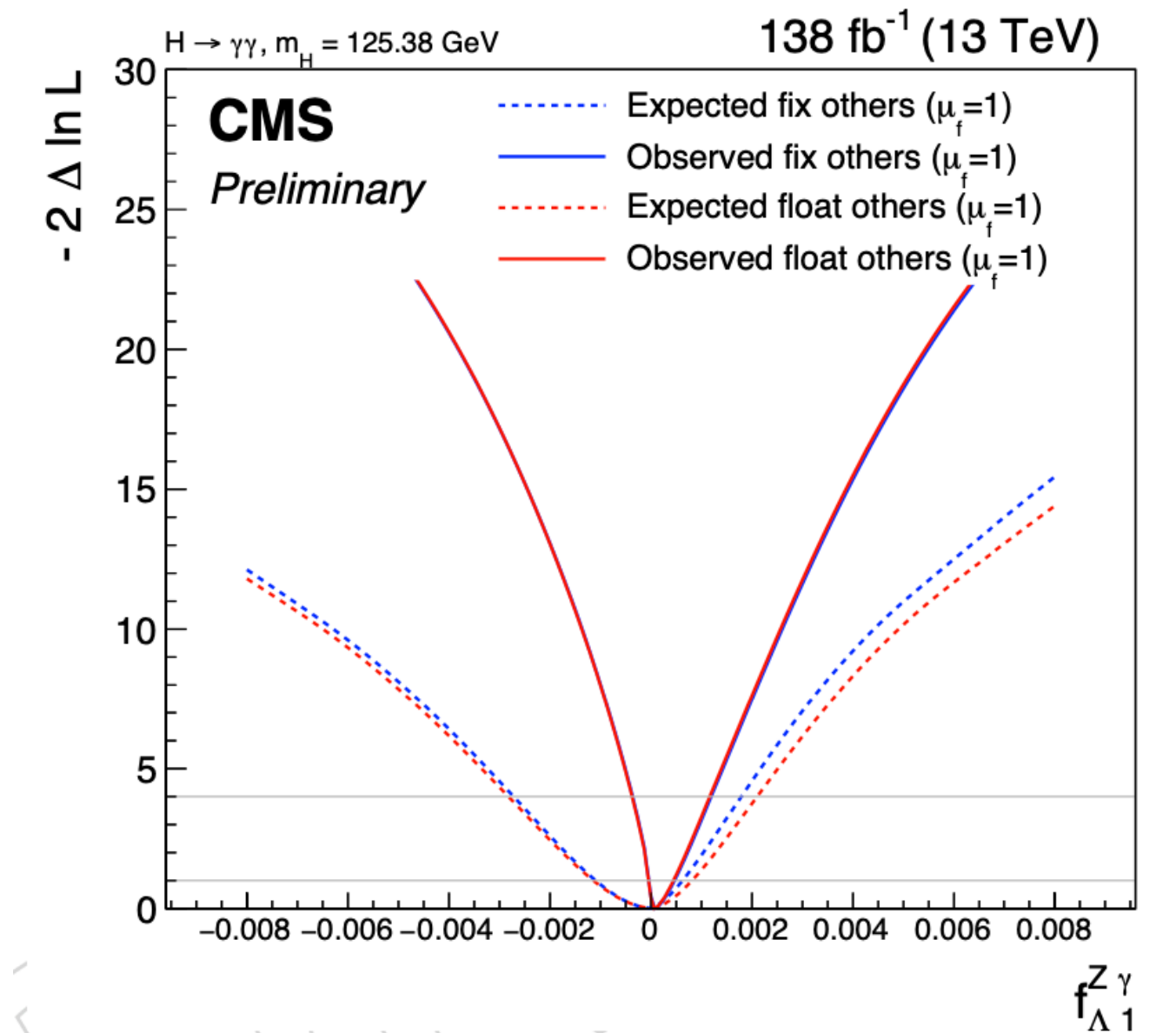
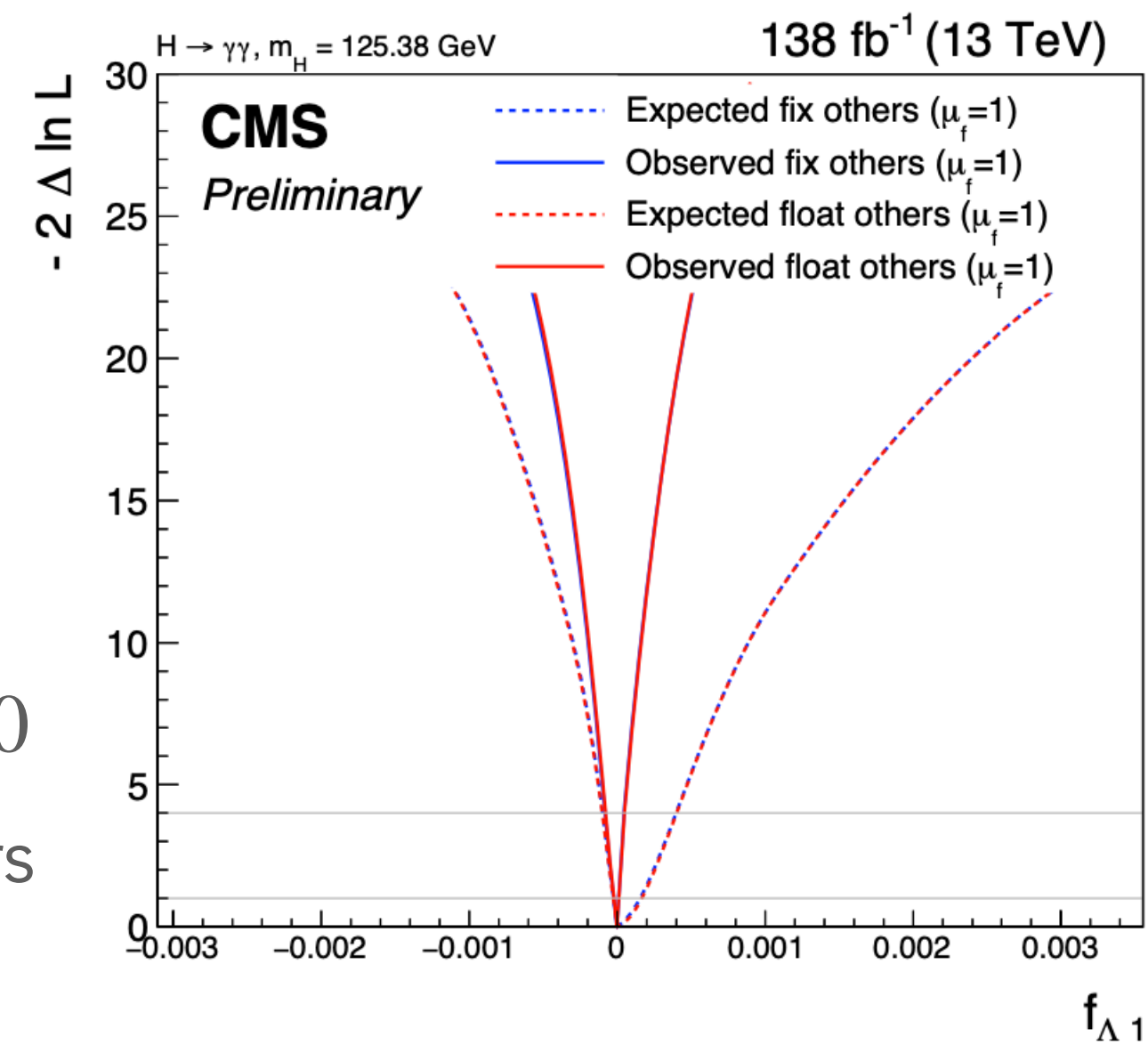
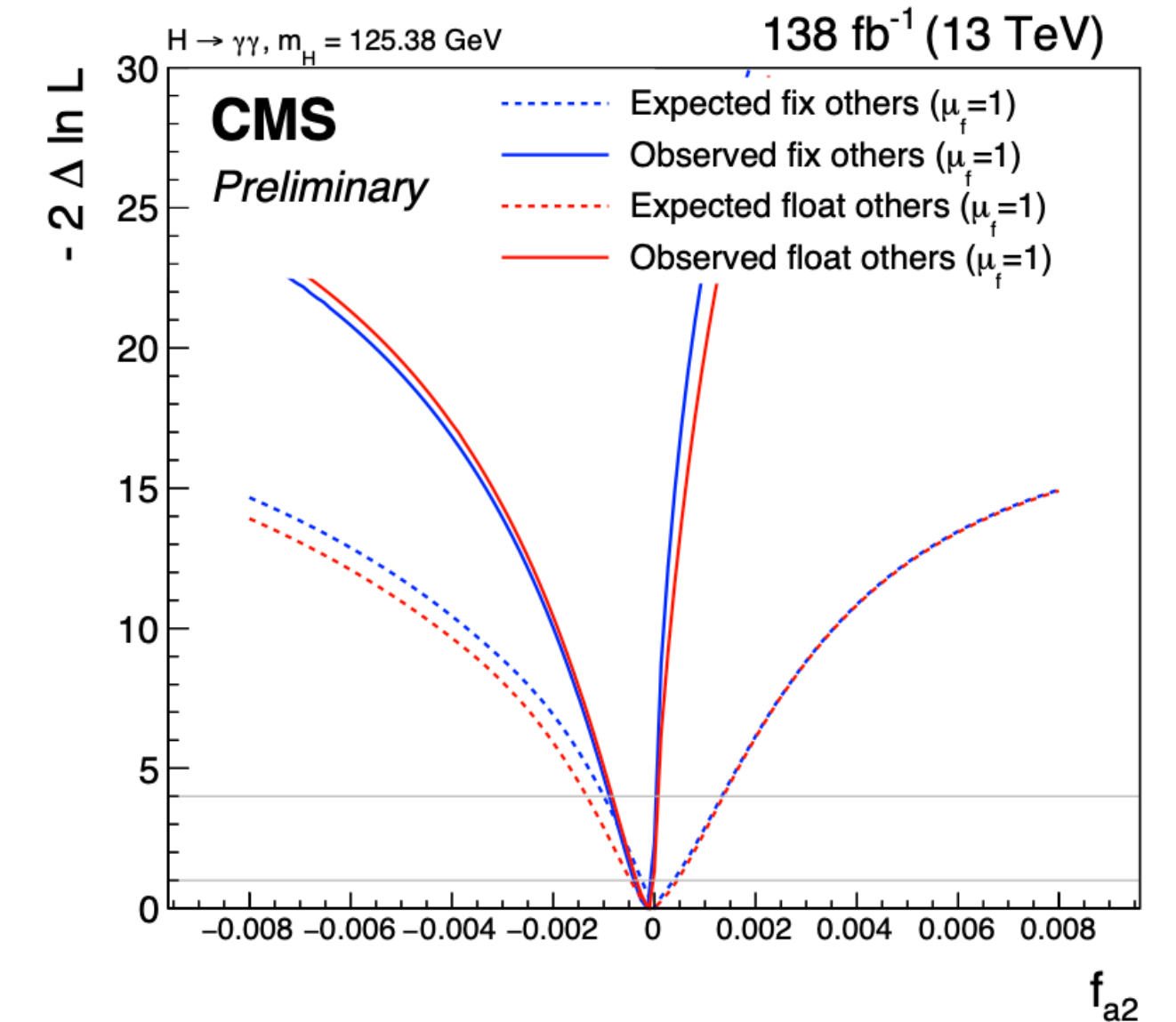
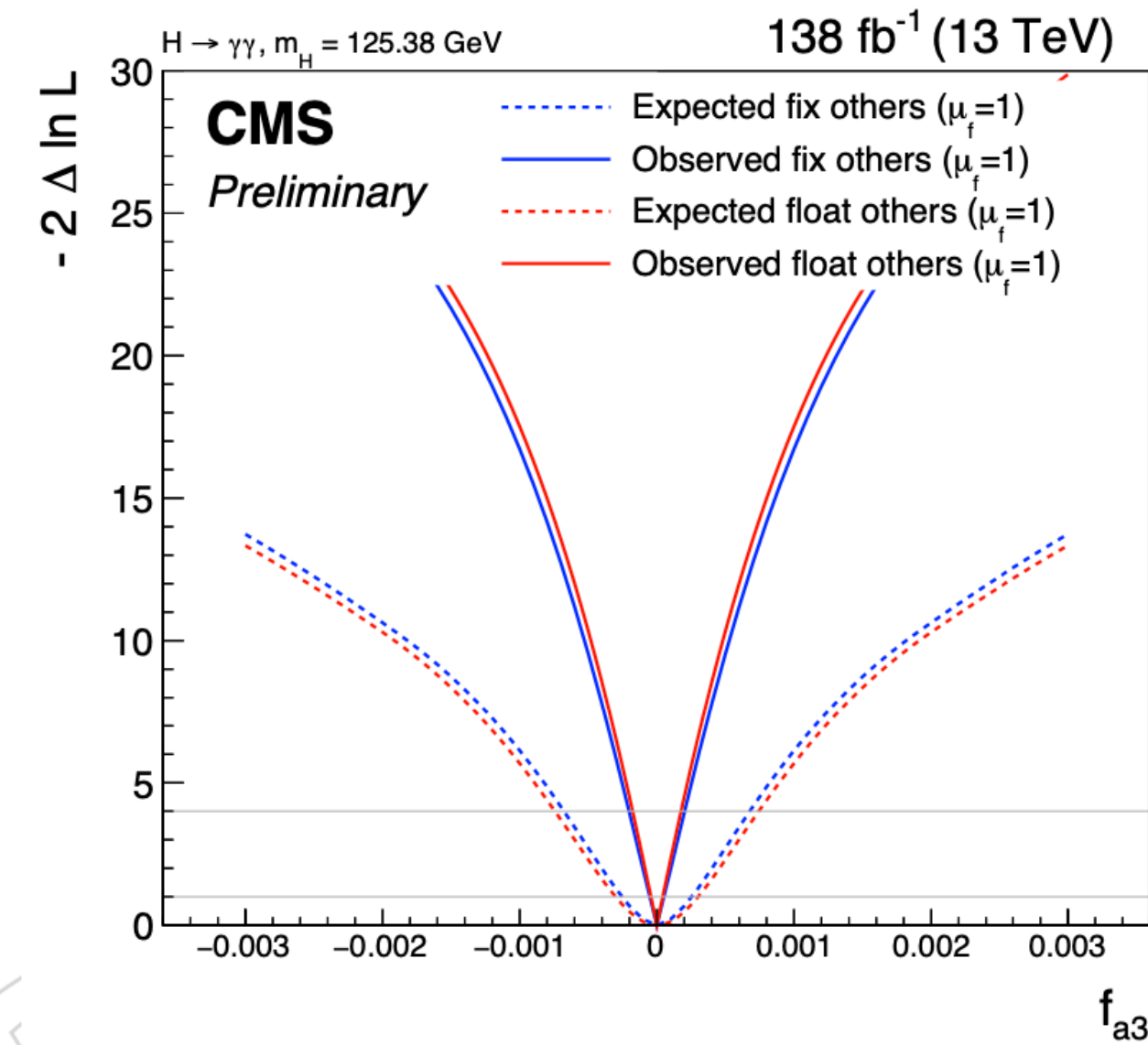
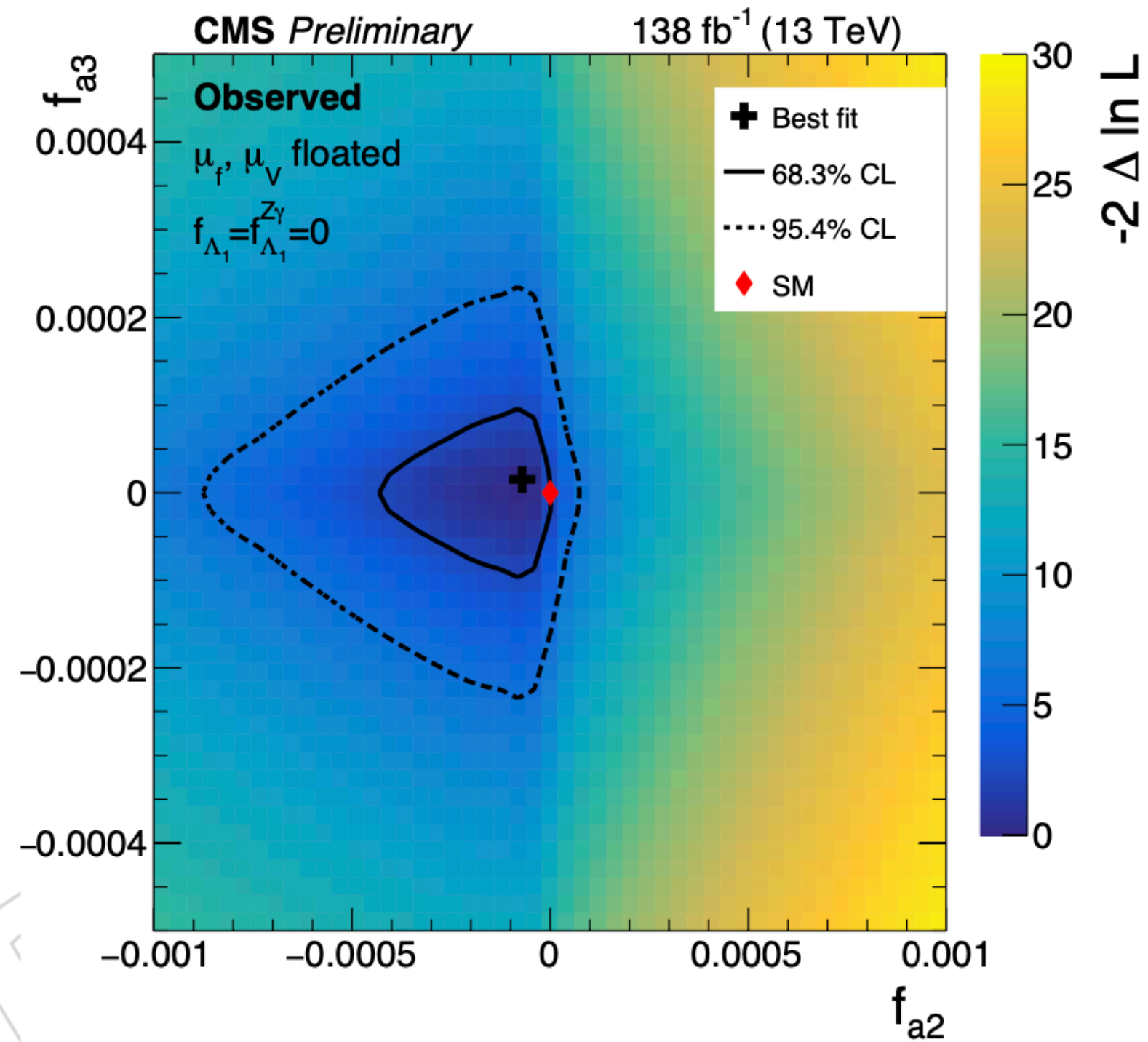


The distribution of events

weighted by $\frac{S^{SM}}{S^{SM} + B}$.

The background contribution, estimated from the sideband fit on data, has been subtracted. The plot displays the comparison with the predicted Higgs signal yield with $f_{a3}=0$; $f_{a3}=1$

Floated scans



Fix others: only one of $f_{ai} \neq 0$

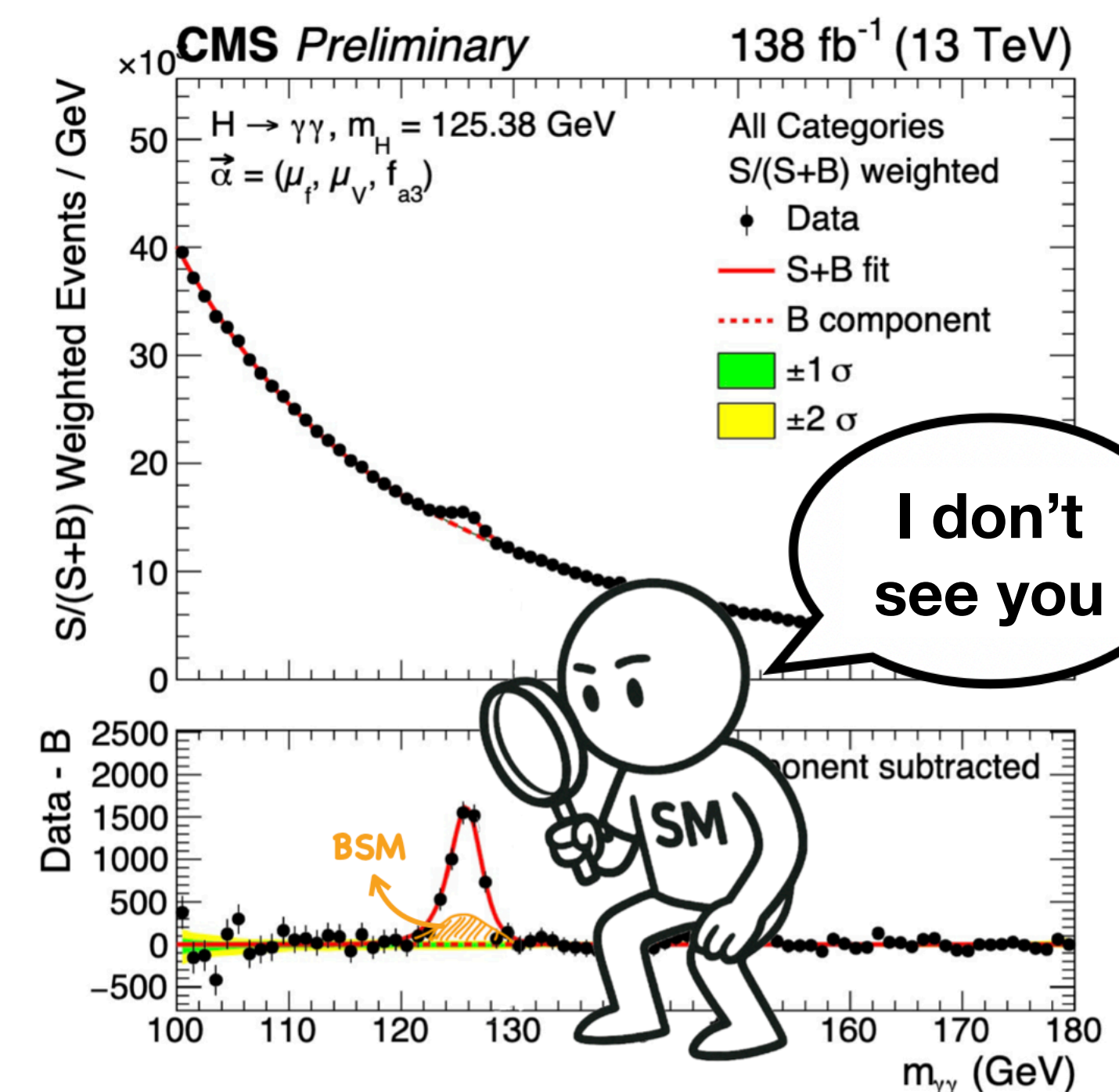
Float others: all f_{ai} free parameters

Summary and conclusion

- ▶ Higgs boson candidates decaying into two photons are analyzed to probe CP-violating effects in both electroweak (VBF and VH) and gluon fusion production mechanisms fitting one AC (most stringent) at a time or floating all simultaneously (more model independent)
- ▶ **No significant deviations from the Standard Model predictions are observed.** The CP-odd effective fraction in gluon fusion production is measured to be $f_{a3}^{ggH} = 0.45^{+0.47}_{-0.43}$ at 68% confidence level. The CP-Odd effective fractions for electroweak production is constrained to $f_{a3} < 2.1 \times 10^{-4}$ at 68% confidence level.
- ▶ These results are compatible with previous measurements in other Higgs decay channels

- ▶ Rapidly growing field with recent advances and possibilities for new interpretations
- ▶ Analyses are limited by statistical uncertainties, so we expect improvements from the increase in data.

Thanks for the attention!





Systematics

$$P_{jk}^{sig}(m_{\gamma\gamma}; \overrightarrow{\theta}_{jk}, f_i) = (1 - f_i)P_{jk}^{a_1}(m_{\gamma\gamma}; \overrightarrow{\theta}_{jk}) + f_i P_{jk}^i(m_{\gamma\gamma}; \overrightarrow{\theta}_{jk}) + 2\sqrt{f_i(1 - f_i)}\cos(\phi_{ai})P_{jk}^{a_1, a_i}(m_{\gamma\gamma}; \overrightarrow{\theta}_{jk})$$

Systematic uncertainties based on the standard $H \rightarrow \gamma\gamma$ analysis

Experimental Uncertainties Affecting Signal Line Shape

15% of the total
systematics unc

- Integrated luminosity
- Photon identification BDT score
- Jet energy scale and smearing corrections
- Per-photon energy resolution estimate
- Trigger efficiency
- Photon preselection
- Pileup jet identification

Experimental Uncertainties Affecting Normalizations

5% of the total
systematics unc

- Photon energy scale and resolution
- Non-linearity of the photon energy scale
- Shower shape corrections
- Non-uniformity of light collection
- Modelling of material in front of the ECAL
- Vertex assignment

Theoretical Uncertainties Affecting Normalizations

- QCD scale uncertainty
- Uncertainties in the ggH contamination
- Uncertainties in the qqH signal fraction
- PDF (parton density functions) uncertainties
- Uncertainty in the strong force coupling constant
- Uncertainty in the $H \rightarrow \gamma\gamma$ branching fraction
- Underlying event and parton shower uncertainties

For **HVV** 20%
of the total
systematics unc

The systematic uncertainties have a limited impact, contributing less than 10% to the total uncertainty.

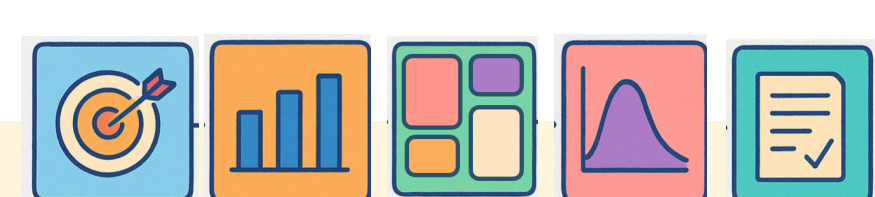
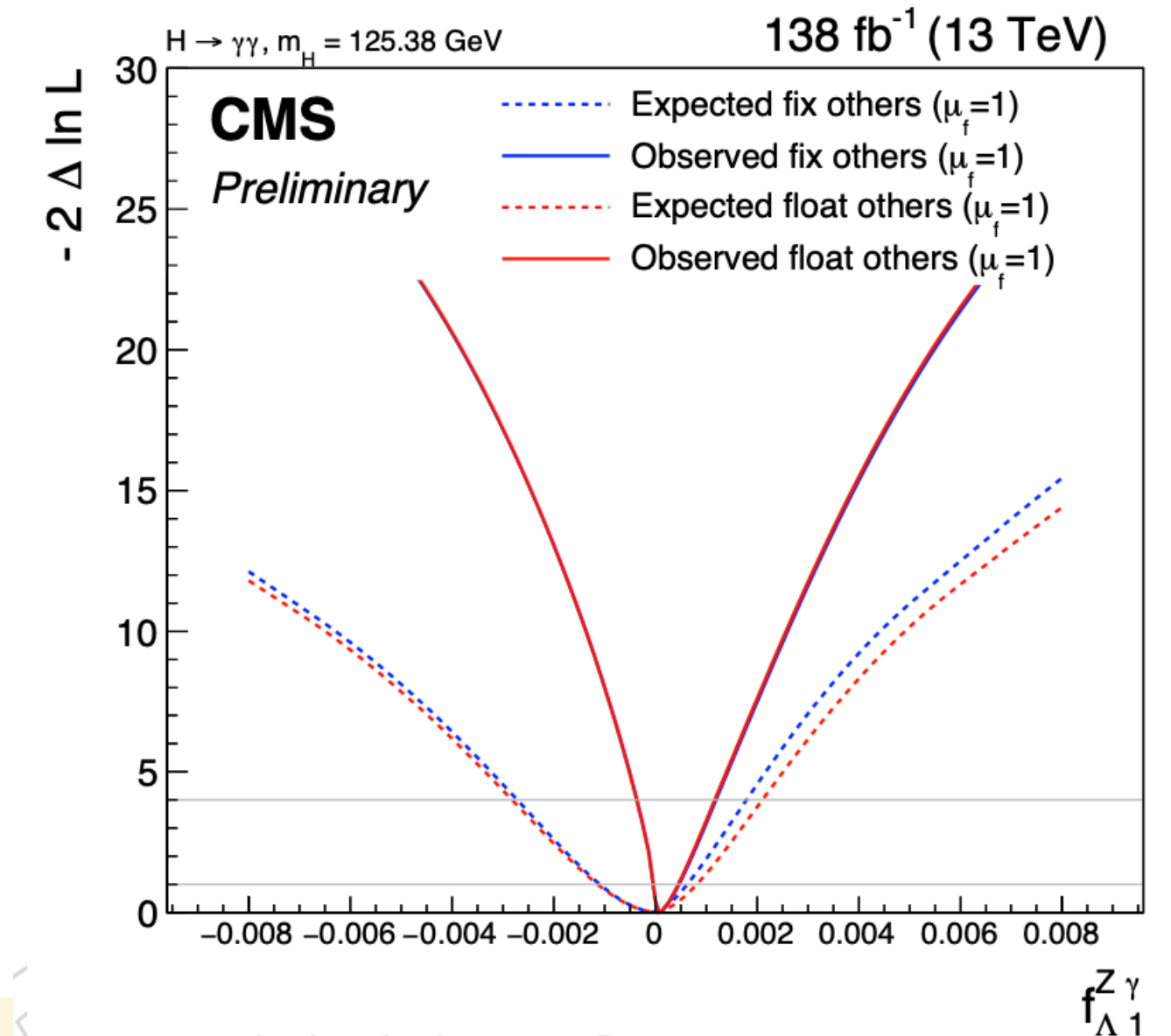
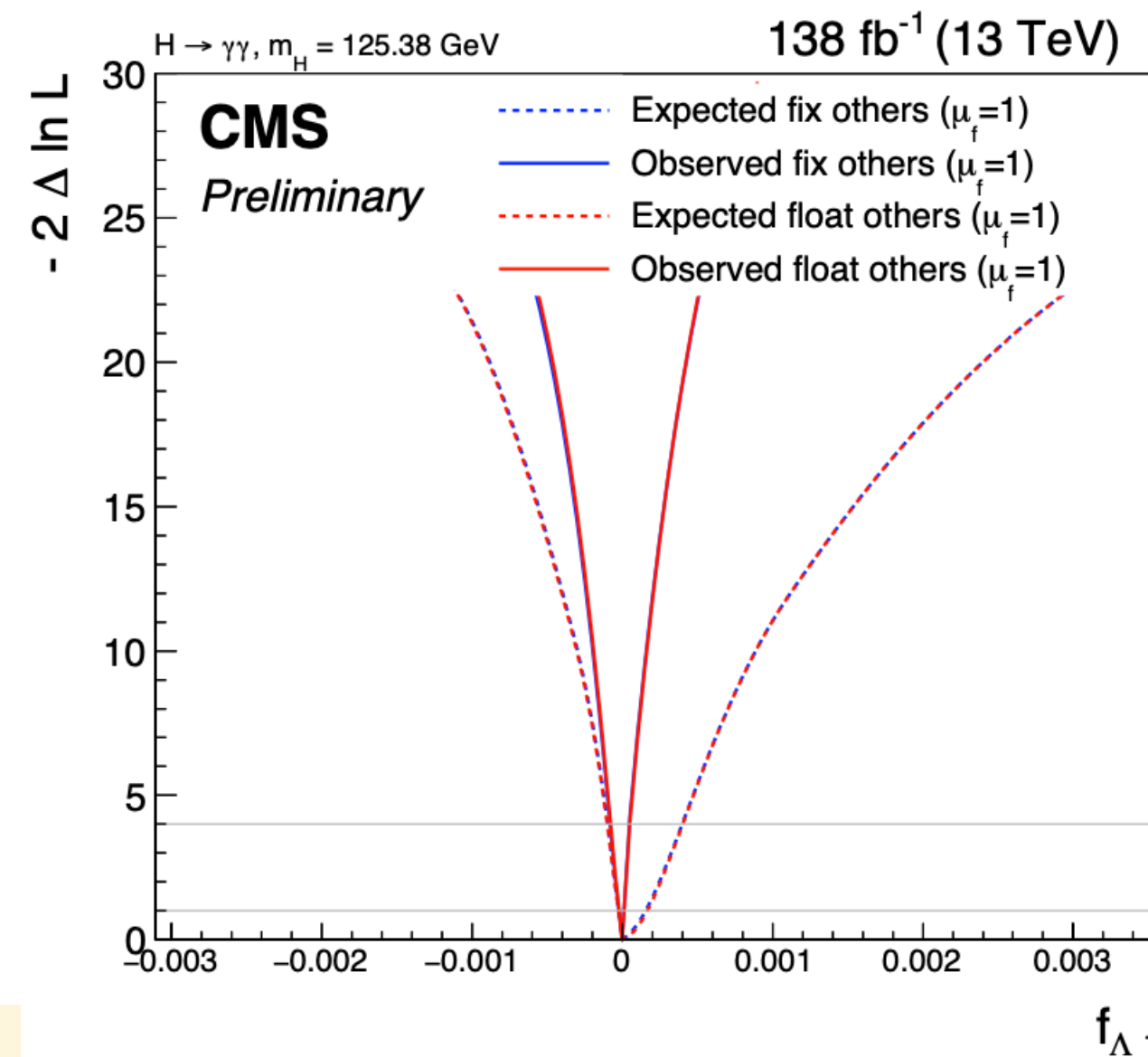
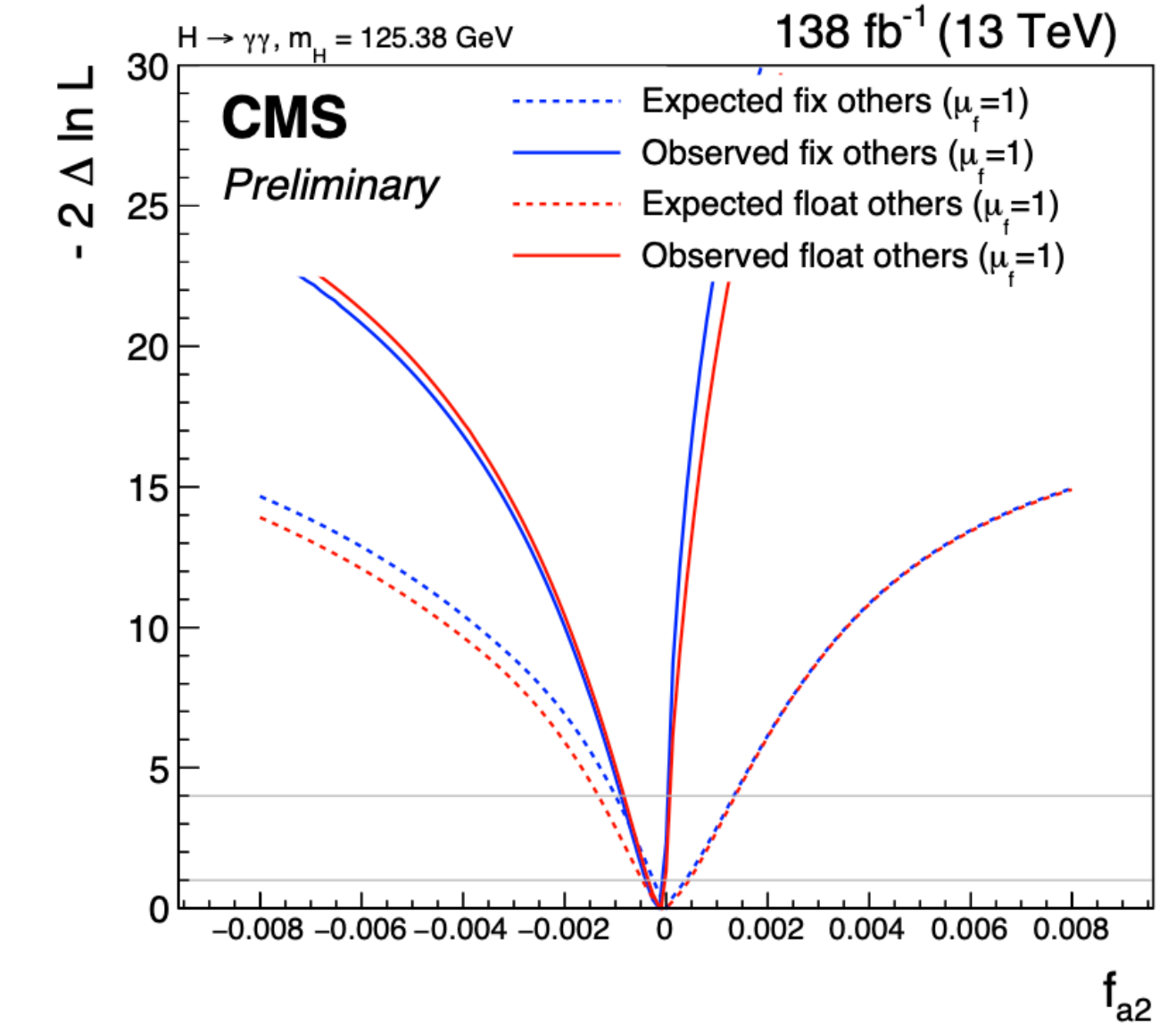
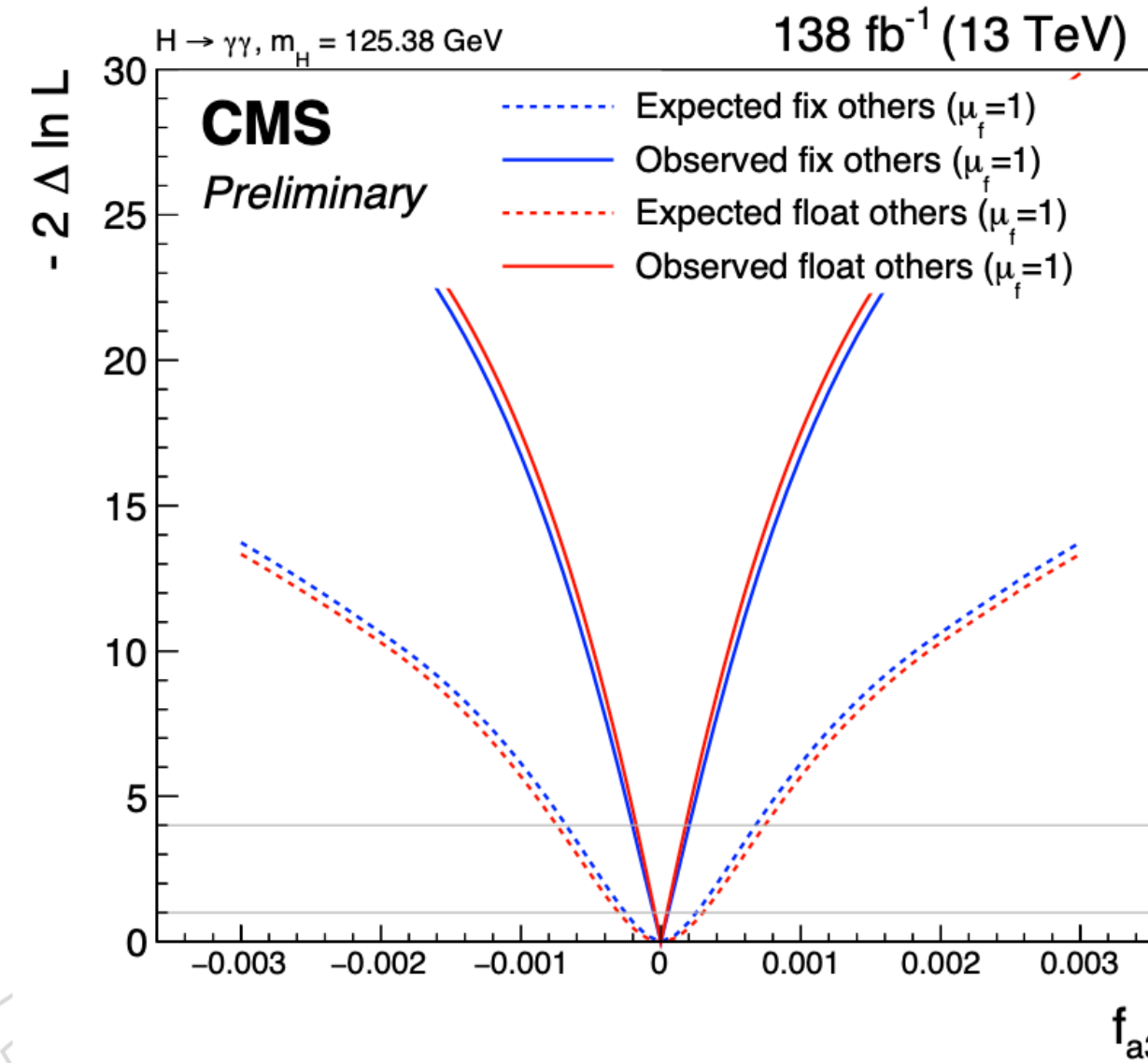


Floated scans

f_{a3}	68 % CL Interval [$\times 10^{-4}$]	95 % CL Interval [$\times 10^{-4}$]
Expected fix others ($\mu_f = 1$)	$0.0^{+2.5}_{-2.5}$	$[-6.8, 6.8]$
Observed fix others ($\mu_f = 1$)	$0.0^{+0.52}_{-0.52}$	$[-2, 2]$
Expected float others ($\mu_f = 1$)	$0.0^{+3.0}_{-3.0}$	$[-7.4, 7.4]$
Observed float others ($\mu_f = 1$)	$0.0^{+0.43}_{-0.43}$	$[-1.8, 1.8]$
f_{a2}	68 % CL Interval [$\times 10^{-4}$]	95 % CL Interval [$\times 10^{-4}$]
Expected fix others ($\mu_f = 1$)	$-0.0^{+3.8}_{-2.5}$	$[-10, 13]$
Observed fix others ($\mu_f = 1$)	$-1.4^{+0.94}_{-2.6}$	$[-7.5, 1.7]$
Expected float others ($\mu_f = 1$)	$-0.029^{+4.5}_{-4.7}$	$[-13, 14]$
Observed float others ($\mu_f = 1$)	$-0.98^{+0.82}_{-2.5}$	$[-7.3, 1.6]$
$f_{\Lambda 1}$	68 % CL Interval [$\times 10^{-4}$]	95 % CL Interval [$\times 10^{-4}$]
Expected fix others ($\mu_f = 1$)	$0.0^{+1.6}_{-0.26}$	$[-0.99, 4.0]$
Observed fix others ($\mu_f = 1$)	$-0.0^{+0.12}_{-0.2}$	$[-0.78, 0.49]$
Expected float others ($\mu_f = 1$)	$0.0^{+1.7}_{-0.27}$	$[-1.0, 4.0]$
Observed float others ($\mu_f = 1$)	$-0.0^{+0.19}_{-0.12}$	$[-0.75, 0.51]$
$f_{\Lambda 1}^{Z\gamma}$	68 % CL Interval [$\times 10^{-4}$]	95 % CL Interval [$\times 10^{-4}$]
Expected fix others ($\mu_f = 1$)	$0.0^{+6.3}_{-11}$	$[-27, 18]$
Observed fix others ($\mu_f = 1$)	$0.7^{+3.9}_{-0.88}$	$[-4.4, 11]$
Expected float others ($\mu_f = 1$)	$0.0005^{+8.1}_{-11}$	$[-28, 21]$
Observed float others ($\mu_f = 1$)	$0.66^{+3.8}_{-0.88}$	$[-4.4, 11]$

Fix others: only one of $f_{ai} \neq 0$

Float others: all f_{ai} free parameters



RESULTS

Trigger & event Selection

Standard HLT trigger for H->γγ is applied

The same branch of the *flashgg* framework is used to reconstruct and select diphoton events in both analyses.

- 2016: HLT_Diphoton30_18_R9Id_OR_IsoCaloId_AND_HE_R9Id_Mass90*
- 2017: HLT_Diphoton30_22_R9Id_OR_IsoCaloId_AND_HE_R9Id_Mass90*
- 2018: HLT_Diphoton30_22_R9Id_OR_IsoCaloId_AND_HE_R9Id_Mass90*

diphoton preselection

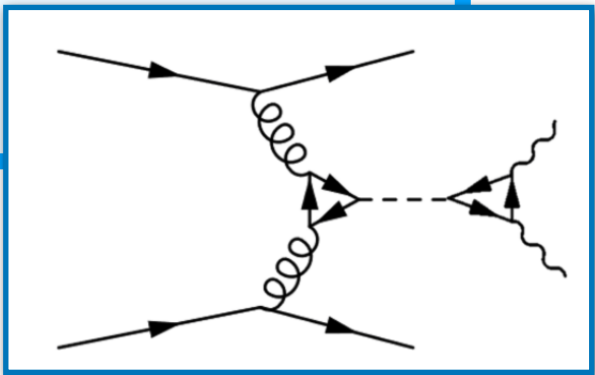
$$|\eta_{1,2}| < 2.5, p_T/m_{\gamma\gamma} > 1/3(1/4)$$

	H/E	$\sigma_{i\eta i\eta}$	R_9	Iso_{ph}	Iso_{track}
EB; $R_9 > 0.85$	< 0.08	–	–	–	–
EB; $R_9 \leq 0.85$	< 0.08	< 0.015	> 0.5	$< 4.0 \text{ GeV}$	$< 6.0 \text{ GeV}$
EE; $R_9 > 0.90$	< 0.08	–	–	–	–
EE; $R_9 \leq 0.90$	< 0.08	< 0.035	> 0.8	$< 4.0 \text{ GeV}$	$< 6.0 \text{ GeV}$
Other preselection requirements					
leading photon $p_T > 35 \text{ GeV}$	$R_9 > 0.8 \text{ OR } Iso_{ch} < 20 \text{ GeV OR } Iso_{ch}/p_T < 0.3$				
sub-leading photon $p_T > 25 \text{ GeV}$					
	$m_{\gamma\gamma} > 100 \text{ GeV}$				

Hgg Analysis focus on events where the **Higgs boson is produced via gluon fusion** in association with **two jets** (ggH + 2 jets), radiated from the initial partons.

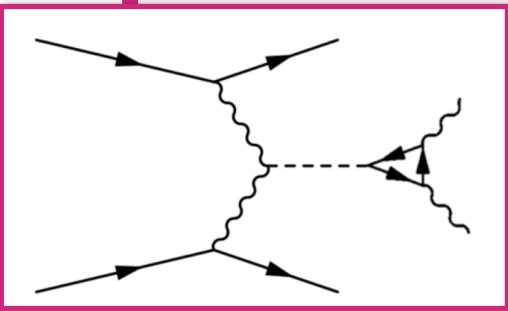
This region of phase space provides **maximal sensitivity** to **anomalous ggH couplings**.

2 Jets selection:
 At leas two jets with $p_T^{1,2} > 30 \text{ GeV}$, $|\eta^{1,2}| < 4.7$, **No m_{jj} cut**
 pohotonID MVA>-0.2, $100 \text{ GeV} < m_{\gamma\gamma} < 180 \text{ GeV}$



ggH

HVV analysis uses similar **STXS (Simplified Template Cross Sections) REF phase space** to better constrain the **resonant background**, especially the ggH production mode.



VBF

